Annex No.4 Reservoir Sedimentation Analysis

THE STUDY ON
COUNTERMEASURES FOR SEDIMENTATION
IN
THE WONOGIRI MULTIPURPOSE DAM RESERVOIR
IN
THE REPUBLIC OF INDONESIA

FINAL REPORT

SUPPORTING REPORT I

Annex No.4: Reservoir Sedimentation Analysis

Table of Contents

List of Tables

List of Figures

CHAPTER 1 INTRODUCTION

In alluvial river course, erosion and/or deposition of riverbed are first initiated by the imbalance of flow and sediment transport. When a reservoir (dam) is constructed in a river, the characteristic balance on flow and sediment transport in the river will be inevitably destroyed. In reservoir, sediment usually deposits because water depth is deeper and flow velocity is slower than those in the river, until an equilibrium state, in which the rate of sediment supplied to the reservoir is balanced by the rate of transport out of the area, is reached. This process results in sedimentation in reservoir. Therefore, a reservoir stores not only water, but also sediment that is transported commonly together with the water flow. Ultimately, such sedimentation may completely fill the reservoir unless adequate mitigation countermeasures are taken.

In this case, due to the Wonogiri dam, the characteristic balance on flow and sediment transport of the Solo River has been destroyed, which resulted in serious sedimentation in the reservoir during the past 25 years. The initial storage capacity in the Wonogiri reservoir was about 7.3×10^8 m^3, the sedimentation volume during past 25 years has reached to about 1×10^8 m^3 and the situation is deteriorating.

The sedimentation reduces effective storage capacity of the reservoir and results in loss of its functions, e.g., water supply, hydropower generation, flood control, and so on. In order to take mitigation countermeasures against sedimentation phenomenon in reservoir, it is important to evaluate current situation of sedimentation and to predict its future change in the reservoir. A sediment transport model is a right tool to predict the reservoir sedimentation because the phenomenon is one kind of bed deformation (Suzuki *et al*, 2004[1]). By the model, transport volume and distribution of sedimentation in reservoir and effect of mitigation countermeasures against sedimentation can be evaluated.

Herein, in order to evaluating the effect of countermeasures against the sedimentation phenomenon, a depth-integrated two-dimensional numerical analysis model, based on a sediment transport model, was developed to study the flow condition and potential of sedimentation in the Wonogiri reservoir under different conditions.

By using the measured data of sedimentation in the reservoir and sediment release from the reservoir, the model was verified first. The results showed that the model can be employed to simulate the sedimentation in the Wonogiri reservoir.

Then the model was applied to predict the effect of proposed mitigation countermeasures against the sedimentation. By the study, an effective mitigation countermeasure, the Compartmented Reservoir with New Gate, has been concluded.

This method is to create a small component reservoir for the sediment inflow form the Keduang River inside the reservoir by installing a closure dike, thereby to allow two reservoir portions to be operated separately. For sediment sluicing during flood in Keduang river, a new gate is installed on right abutment of the dam. Through the new gate, sediment-laden flood inflow from the Keduang River can be passed through before deposition in the reservoir.

By the analyses of sedimentation simulation, the following points are concluded.

[1] Suzuki, T., Kashiwai, J., and Yoshioka, Y. (2004). "Estimation of Nonuniform Sediment Discharge Using Actual Results of Dam Reservoir Sedimentation". *Dam Engineering*, JSDE. Vol.14, No.4, pp.257-269.

- The sediment release efficiency by the Compartmented Reservoir with New Gate under the new operation rule is quite higher. In both hydrological average year and flood year, volume of sediment release reaches to around 1 million m^3.
- Sedimentation in the area around the intake becomes slightly.
- Under the new operation rule, the reservoir water level can be kept at higher level by the end of the rainy season in all hydrological years. Therefore, it could be understood that the water use by the new sediment flushing gate is normally released from the reservoir according to the dam operation rule for the safety of the dam.
- At the crest level 127m, the efficiency of sediment release decreases a lot if the width of new gate reduces from 15m to 10m. Wider than the width 15m of the gate, variation of the efficiency is not so greater.
- The efficiency reduces a lot if the crest level is raised to 128 m, even the same gate width 15m is set.

Therefore, from the viewpoint of the balance between cost and benefit, it is recommended that the width and the crest level of new sediment flushing gate are set to 15m and 127m.

CHAPTER 2 RESERVOIR SEDIMENTATION ANALYSIS MODEL

Reservoir sedimentation is one kind of river bed deformation phenomenon, in which sediment deposition is dominant. In the Wonogiri reservoir, transport of very fine sediment, i.e., washload, which is usually clay and silt, is dominant due to slower flow. The finer sediment is generally supplied by sheet erosion in upland area.

Primary purpose of modeling, both numerically and physically, is to mirror 'exactly' or duplicate the phenomena on compressed scale that cannot be, or difficult to be, observed in prototype. In this case, because of the domination of very finer sediment in transportation, it is quite difficult to do a physical model test due to limitation on the scale similarity. A numerical method can provide an advantage in evaluating such extreme conditions with the same temporal and spatial scales.

In many situations, reservoir water can be considered as shallow waters. In the Wonogiri reservoir, maximum surface area of is about 88km^2. The water depth is shallow and its maximum is now less than 18m when the water level is at the normal level (136 m). Therefore a depth-integrated two-dimensional model is appropriate for evaluating flow condition and sedimentation in the Wonogiri reservoir because of its wider and shallower features of the domain.

2.1 Boundary-Fitted Orthogonal Curvilinear Coordinate System

Planform of the Wonogiri reservoir is complicated with some coves and inflow tributaries. A model based on a boundary-fitted curvilinear coordinate system is preferable for analyzing the reservoir sedimentation phenomenon.

Conventional Cartesian grids have been used and are now still used to solve Computational Fluid Dynamics (CFD) problems. A disadvantage to this approach, however, is that the irregular physical boundaries have to be represented in a 'staircase fashion' (Fig.2.1.1(a)). A new and very promising approach is to generate curvilinear grids that conform to the boundaries (Fig.2.1.1(b)). There are coordinate lines in such a coordinate system to overlap the domain boundaries completely, similar to a cylindrical and a spherical coordinate for circular and spherical regions respectively, etc. Such a system is preferable when the boundary conditions and numerical scheme are applied. Furthermore, computational grid in curvilinear coordinate system is flexible in grid size, by which effective simulation for long-term phenomenon becomes possible.

Image of the coordinate transformation is shown in Figure 2.1.2.

Herein a depth-integrated two-dimensional numerical model, NKhydro2D sediment transport model developed by Nippon Koei Co., Ltd., is employed. The model is based on numerically generated boundary-fitted orthogonal curvilinear grids. The definition of boundary-fitted orthogonal coordinates in river course is shown in Fig.2.1.3. Incorporated with the information on area configuration, bed elevation and its material (sediment), hydraulic structure, water inflow and outflow, sediment supply (inflow) and release (outflow), and other hydraulics and meteorological conditions, various problems in the waters can be studied and analyzed by the Nkhydro2D model. By comparing the simulation results with laboratory and field data, reliability of the model has been verified. Moreover, for applying the model to the Wonogiri reservoir, the model is also verified by corresponding survey data in the following simulations.

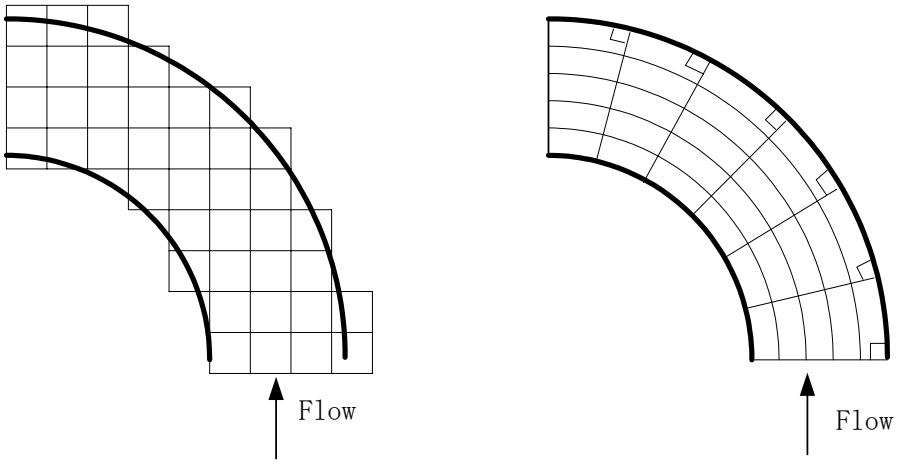

(a) In Cartesian Coordinates (b) In Curvilinear Orthogonal Coordinates

Figure 2.1.1 Computational Grid System

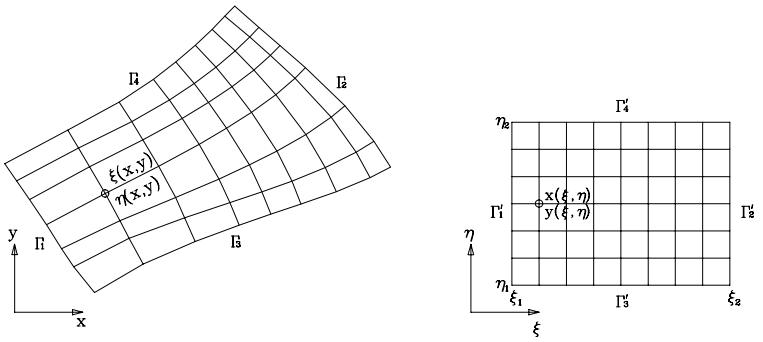

(a) In physical space (b) In transformed space

Figure 2.1.2 Coordinate Transformation

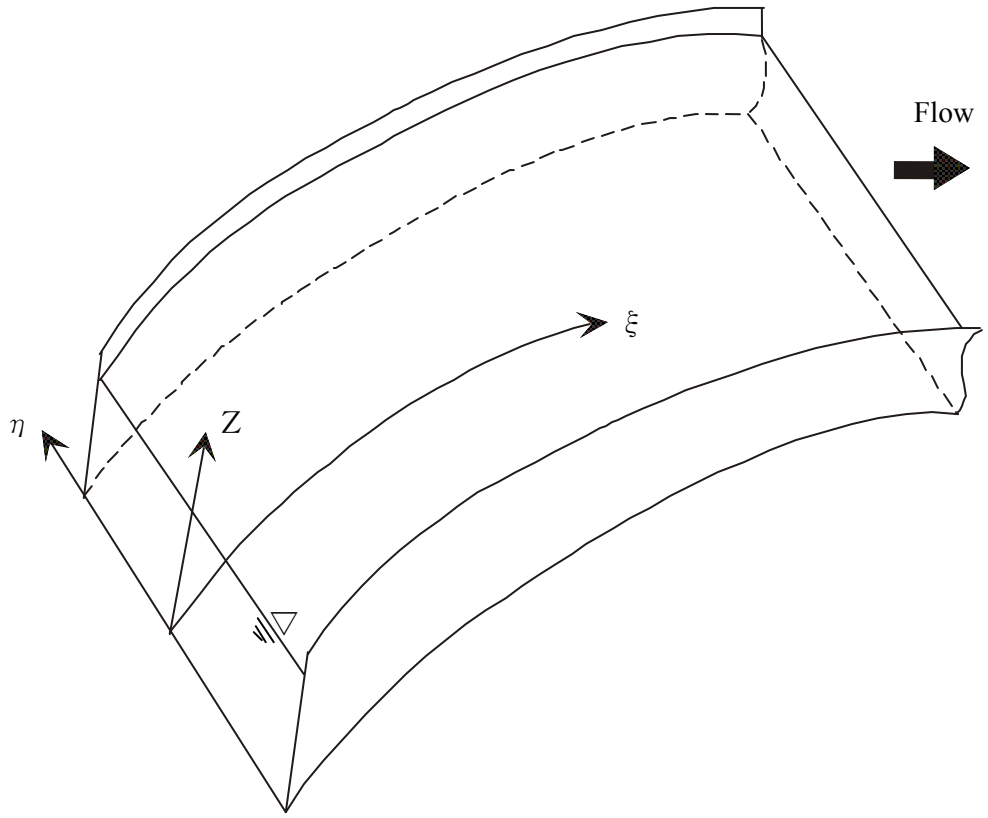

Figure 2.1.3 Definition of Curvilinear Orthogonal Coordinate System in River Course

2.2 Governing Equations

In the present model, depth-integrated two-dimensional (2D) Reynolds' equations for water flow and advection-diffusion equation for suspended sediment concentration are solved by a control volume method based finite difference scheme. Both the sediment settling to bed and the entrainment from bed are taken into account in evaluating the sediment transport and sedimentation (bed deformation). The non-uniformity of sediment (both in bed material and in suspended sediment) is considered in the simulations.

Governing equations are expressed in orthogonal curvilinear coordinate system. Assuming constant density and hydrostatic pressure variations and using the Boussinesq's approximate for turbulent stresses, the equations are written as follows.

2.2.1 Governing Equations for Water Flow

Continuity equation

$$\frac{\partial h}{\partial t}+\frac{1}{g_{11}g_{22}}\left[\frac{\partial(u^{*}hg_{22})}{\partial\xi}+\frac{\partial(v^{*}hg_{11})}{\partial\eta}\right]=0 \qquad (2.1)$$

ξ-Momentum equation

$$\begin{aligned}&\frac{\partial(hu^*)}{\partial t}+\frac{1}{g_{11}g_{22}}[\frac{\partial(g_{22}hu^{*2})}{\partial\xi}+\frac{\partial(g_{11}hu^*v^*)}{\partial\eta}\\&+h(u^*v^*\frac{\partial g_{11}}{\partial\eta}-v^{*2}\frac{\partial g_{22}}{\partial\xi})]=-\frac{hg}{g_{11}}\frac{\partial\zeta}{\partial\xi}\\&+\frac{1}{g_{11}g_{22}}[\frac{\partial(hg_{22}\sigma_1^*)}{\partial\xi}+\frac{\partial(hg_{11}\tau_{21}^*)}{\partial\eta}+h(\tau_{12}^*\frac{\partial g_{11}}{\partial\eta}\\&-\sigma_2^*\frac{\partial g_{22}}{\partial\xi})]+\frac{\tau_{s\xi}-\tau_{b\xi}}{\rho}+fhv^*\end{aligned}\qquad (2.2)$$

η-Momentum equation

$$\begin{aligned}&\frac{\partial(hv^*)}{\partial t}+\frac{1}{g_{11}g_{22}}[\frac{\partial(g_{22}hu^*v^*)}{\partial\xi}+\frac{\partial(g_{11}hv^{*2})}{\partial\eta}\\&+h(u^*v^*\frac{\partial g_{22}}{\partial\xi}-u^{*2}\frac{\partial g_{11}}{\partial\eta})]=-\frac{hg}{g_{22}}\frac{\partial\zeta}{\partial\eta}\\&+\frac{1}{g_{11}g_{22}}[\frac{\partial(hg_{22}\tau_{12}^*)}{\partial\xi}+\frac{\partial(hg_{11}\sigma_2^*)}{\partial\eta}+h(\tau_{21}^*\frac{\partial g_{22}}{\partial\xi}\\&-\sigma_1^*\frac{\partial g_{11}}{\partial\eta})]+\frac{\tau_{s\eta}-\tau_{b\eta}}{\rho}-fhu^*\end{aligned}\qquad (2.3)$$

where ξ and η are the orthogonal curvilinear coordinates in transformed space, u^* and v^* are the ξ and η component of depth-averaged velocity in the orthogonal curvilinear coordinate system respectively.

$$u^*=(u\,x_\xi+v\,y_\xi)/g_{11}\quad,\quad v^*=(u\,x_\eta+v\,y_\eta)/g_{22}\qquad (2.4)$$

u, v are the x and y component of depth-averaged velocity in the Cartesian coordinate system respectively. x, y are the coordinates in the Cartesian coordinate system (physical space).

ζ, h are the water surface level and water depth respectively, $h=\zeta-Z_b$, Z_b is the bed elevation. ρ, g and f are the density of water, gravity acceleration and Coriolis coefficient respectively, g=9.8m/s^2, f=2Ωsinϕ, Ω is the angular velocity of earth rotation, ϕ is the latitude of the interest region. τ_s is the shear stress at the water surface and depends on the wind speed. τ_b is the shear stress at the river bed.

$$\tau_{s\xi}=C_w\rho_a|W|W_\xi\quad,\quad \tau_{s\eta}=C_w\rho_a|W|W_\eta\qquad (2.5)$$

$$\frac{\tau_{b\xi}}{\rho}=C_f u^*\sqrt{u^{*2}+v^{*2}}\quad,\quad \frac{\tau_{b\eta}}{\rho}=C_f v^*\sqrt{u^{*2}+v^{*2}}\qquad (2.6)$$

W_ξ and W_η are the ξ and η component of the wind speed W (m/s), ρ_a (kg/m^3) is the air density, C_W is the drag (friction) coefficient of the wind. Usually the drag coefficient is a function of the measurement height above the water surface. Most drag coefficient formulae

have been determined based on a 10m wind speed measurement height. The drag coefficient based on a 10m measurement height, C_W, is defined as:

$$C_W = \begin{cases} 0.0, & for \quad W < 1\,m/s \\ 0.0005W^{0.5}, & for \quad 1 \le W < 15\,m/s \\ 0.0026, & for \quad W \ge 15\,m/s \end{cases} \tag{2.7}$$

C_f ($= n^2 g / h^{1/3}$) is the resistance coefficient, n is the Manning's roughness coefficient.

σ_1^*, σ_2^*, τ_{12}^* and τ_{21}^* are the depth-averaged Reynolds' shear stresses (Rodi 1980[2]).

$$\sigma_1^* = 2\nu_t\left[\frac{1}{g_{11}}\frac{\partial u^*}{\partial \xi} + \frac{v^*}{g_{11}g_{22}}\frac{\partial g_{11}}{\partial \eta}\right] \tag{2.8}$$

$$\sigma_2^* = 2\nu_t\left[\frac{1}{g_{22}}\frac{\partial v^*}{\partial \eta} + \frac{u^*}{g_{11}g_{22}}\frac{\partial g_{22}}{\partial \xi}\right] \tag{2.9}$$

$$\tau_{12}^* = \tau_{21}^* = \nu_t\left[\frac{1}{g_{11}}\frac{\partial v^*}{\partial \xi} + \frac{1}{g_{22}}\frac{\partial u^*}{\partial \eta} - \frac{u^*}{g_{11}g_{22}}\frac{\partial g_{11}}{\partial \eta} - \frac{v^*}{g_{11}g_{22}}\frac{\partial g_{22}}{\partial \xi}\right] \tag{2.10}$$

In accordance with Taylor's analysis, ν_t is a product of the Lagrangian length scale (a measure of how far a particle travels before it forgets its initial velocity) and the turbulence intensity. Experiments by Laufer and others have shown that turbulence intensity in any wall shear flow in regular system is proportional to the shear stress on the wall. The shear stress can be represented by friction (shear) velocity. On the other hand, the water depth can be identified with the relevant length scale. Clearly present knowledge on ν_t is inadequate and so a simple empirical formula, $\nu_t = \alpha h u_*$, is usually used to calculate ν_t in natural water bodies, in which α is the dimensionless eddy viscosity coefficient and was estimated to be 0.6, herein, u_* is the friction velocity. $u_* = \sqrt{\tau_b/\rho} = [C_f(u^{*2} + v^{*2})]^{1/2}$.

g_{11} and g_{22} are the orthogonal curvilinear coordinate transformation relationship.

$$g_{11} = \sqrt{x_\xi^2 + y_\xi^2}\ , \quad g_{22} = \sqrt{x_\eta^2 + y_\eta^2} \tag{2.11}$$

$$x_\xi = \frac{\partial x}{\partial \xi}\ ,\ x_\eta = \frac{\partial x}{\partial \eta}\ ,\ y_\xi = \frac{\partial y}{\partial \xi}\ ,\ y_\eta = \frac{\partial y}{\partial \eta} \tag{2.12}$$

2.2.2 Governing Equation for Sediment Transport

River (reservoir) bed deformation (sedimentation) is calculated by mass conservation equation for sediment transport, which is expressed as:

$$\frac{\partial Z_b}{\partial t} + \frac{1}{1-\lambda}\frac{1}{g_{11}g_{22}}\left[\frac{\partial}{\partial \xi}(g_{22}q_{s\xi}) + \frac{\partial}{\partial \eta}(g_{11}q_{s\eta})\right] = 0 \tag{2.13}$$

[2] Rodi, W. (1980). *Turbulence models and their application in hydraulics*. IAHR Publication, DELFT, The Netherlands.

where λ is the porosity of bed material, $q_{s\xi}$ and $q_{s\eta}$ are the ξ and η components of volumetric sediment transport rate. q_s consists of bedload transport rate (q_b) and suspended load one (q_{ss}).

In this case, bedload transport in deeper and wider area may be neglected, but it is important in river area. On the other hand, in deeper and wider area of the reservoir, suspended load is absolutely dominant in the sediment transport.

Non-uniformity of sediment in both the bed material and the suspended sediment (load) is considered because the sampling analyses of both the bed material and the suspended sediment showed that the sediment in the reservoir is quite non-uniform and its diameter ranges from μm to cm.

(1) Bedload Transport

According to local hydraulic conditions, the bedload transport rate q_b is evaluated by selected formula, herein, Ashida-Michiue's formula (Ashida and Michiue 1971)[3]. For non-uniform sediment, the bedload transport rate of k-class sediment, q_{bk}, is calculated as follows,

$$q_{bk} = 17 p_{bk} \frac{\rho u_{*e}^3}{(\rho_s - \rho)g}(1 - K_c \frac{u_{*ck}^2}{u_*^2})(1 - \sqrt{K_c}\frac{u_{*ck}}{u_*}) \tag{2.14}$$

$$q_b = \sum_k q_{bk}\ ,\ \ q_{b\xi} = \sum_k q_{bk}\cos\beta \ \text{ and } \ q_{b\eta} = \sum_k q_{bk}\sin\beta \tag{2.15}$$

where $q_{b\xi}$ and $q_{b\eta}$ are the ξ and η components of volumetric bedload transport rate. p_{bk} is the percentage weight of particle class with size d_k (diameter). ρ_s is the mass density of sediment particles. u_{*e} is the effective friction velocity at bed. $u_{*e} = U/\{6 + 2.5\ln[h/d_m(1+2\tau_{*m})]\}$, $\tau_{*m} = \rho u_*^2/(\rho_s - \rho)g d_m$. U is the depth-averaged velocity, u_{*ck} is the critical friction velocity related to the reference diameter d_k of bedload. According to the corrected Egiazaroff's formula by Ashida and Michiue, the relationship between the critical friction velocity u_{*ck} for diameter d_k and the critical friction velocity u_{*cm} for mean diameter d_m is as below.

$$\frac{u_{*ck}^2}{u_{*cm}^2} = \begin{cases} \dfrac{d_k}{d_m}\cdot 1.64/\left(\log_{10} 19 d_k/d_m\right)^2, & d_k/d_m \geq 0.4 \\ 0.85, & d_k/d_m < 0.4 \end{cases} \tag{2.16}$$

In the simulation, the critical friction velocity u_{*cm} for mean diameter d_m was first calculated according to the Sheild's diagram, then the critical friction velocity u_{*ck} for diameter d_k was calculated by the above formula (2.16).

β in equation (2.15) is the direction of bedload movement evaluated in terms of both the bottom flow directions (u_b—velocity near bed) related to secondary currents and local bed slope. Secondary currents are fundamental in solving the bed evolution. It is well

[3] Ashida, K., and Michiue, M. (1971). *Study on bed load transportation for non-uniform sediment and riverbed variation*. Annuals of the Disaster Prevention Research Institute, Kyoto University, 14(B), pp.259-273. (in Japanese)

known that its strength is closely related to curvature radius of streamline and flow intensity. Herein the streamlines were calculated according to the resulting depth-integrated velocity field.

K_c is the correction factor due to influence of bed slope,

$$K_c = 1 + \frac{1}{\mu_s}[(\frac{\rho}{\rho_s - \rho} + 1)\cos\alpha \frac{\partial Z_b}{g_{11}\partial\xi} + \sin\alpha \frac{\partial Z_b}{g_{22}\partial\eta}], \qquad \tan\alpha = u_{b\eta}/u_{b\xi} \tag{2.17}$$

μ_s is the static friction coefficient of sediment.

(2) Suspended Load Transport

In deeper area of the reservoir, suspended load is absolutely dominant in the sediment transport. Suspended load transport rate q_{ss} is calculated according to the following depth-integration,

$$q_{ss\xi} = \int_{Z_{Cb}}^{\zeta} u^*(z)C(z)dz, \qquad q_{ss\eta} = \int_{Z_{Cb}}^{\zeta} v^*(z)C(z)dz \tag{2.18}$$

in which $C(z)$ is concentration of suspended load, $u^*(z)$ and $v^*(z)$ are the ξ and η component of velocity. Z_{Cb} ($\approx 0.05h$) is reference level near bed.

Figure 2.2.1 shows schematic vertical distribution of velocity and suspended load concentration. Bed deformation due to suspended load transport occurs by the difference between the entrainment and sedimentation. Bed degradation (erosion) occurs when the entrainment dominates, and conversely aggradation (deposition) occurs when settling is dominant. Sediment entrained from bed is transported according to advection and diffusion mechanism. The depth-averaged concentration of suspended load is estimated by the following equation.

(a) Flow velocity (b) Suspended load concentration

Figure 2.2.1 Schematic Vertical Distribution of Velocity and Concentration

$$\frac{\partial hC}{\partial t} + \frac{1}{g_{11}g_{22}}[\frac{\partial(g_{22}hu^*C)}{\partial\xi} + \frac{\partial(g_{11}hv^*C)}{\partial\eta}] = \frac{1}{g_{11}g_{22}}[\frac{\partial}{\partial\xi}(\frac{g_{22}}{g_{11}}hD_C\frac{\partial C}{\partial\xi}) + \frac{\partial}{\partial\eta}(\frac{g_{11}}{g_{22}}hD_C\frac{\partial C}{\partial\eta})] + (q_{su} - \omega_k C_b)\big|_{bed} \tag{2.19}$$

in which, C and C_b are the depth-averaged concentration and that near bed of suspended load, respectively. D_C ($=\nu_t/\sigma_t$) is the diffusion coefficient, and σ_t is Schmidt/Prandtl number. q_{su} is the entrainment rate of suspended load from the river

(reservoir) bed and is calculated by selected formula, herein, Itakura-Kishi's formula (JSCE 1999) [4].

$$q_{su} = \omega_k C_{beq} \tag{2.20}$$

C_{beq} is the reference concentration near the bed. According to Itakura-Kishi's formula,

$$C_{beq} = K(\alpha_* \frac{1}{1+s} \frac{u_*}{\varpi_k} \frac{\Omega}{\tau_*} - 1) \tag{2.21}$$

$$\Omega = \frac{\tau_*}{B_*} \frac{\int_{a'}^{\infty} \xi \frac{1}{\sqrt{\pi}} \exp(-\xi^2) d\xi}{\int_{a'}^{\infty} \frac{1}{\sqrt{\pi}} \exp(-\xi^2) d\xi} + \frac{\tau_*}{B_* \eta_0} - 1, \quad a' = \frac{B_*}{\tau_*} - \frac{1}{\eta_0}$$

$K = 0.0018$, $\alpha_* = 0.14$, $B_* = 0.143$, $\eta_0 = 0.5$

ω_k is the settling velocity of suspended load with size d_k and is estimated by van Rijn's formula (van Rijn 1984) [5].

$$\omega_k = \begin{cases} \frac{1}{18} \frac{(s-1) g d_k^2}{\nu}, & d_k < 0.1mm \\ 10 \frac{\nu}{d_k} \left\{ \left[1 + \frac{0.01(s-1) g d_k^3}{\nu^2} \right]^{0.5} - 1 \right\}, & 0.1 \le d_k < 1.0mm \\ 1.1 \left[(s-1) g d_k \right]^{0.5}, & d_k \ge 1.0mm \end{cases} \tag{2.22}$$

in which, $s = \rho_s / \rho$=2.65, ν is kinematic viscosity coefficient.

Concentration of suspended load near bed, C_b, is assumed to be a function of depth-averaged concentration C and is calculated as below,

$$C_b = f(C) \cong \frac{\beta_C}{1 - e^{-\beta_C}} C, \quad \beta_C = \frac{\omega_k h}{\varepsilon} \tag{2.23}$$

ε is a depth-averaged diffusion coefficient and according to the Prandtl mixing length theory, $\varepsilon = \frac{\kappa}{6} h u_*$, $\kappa = 0.4$.

Therefore, in reservoir sedimentation analysis, river (reservoir) bed deformation (sedimentation) is calculated as below.

$$\frac{\partial Z_b}{\partial t} + \frac{1}{1-\lambda} \frac{1}{g_{11} g_{22}} \left[\frac{\partial}{\partial \xi} (g_{22} q_{b\xi}) + \frac{\partial}{\partial \eta} (g_{11} q_{b\eta}) \right] = -\frac{1}{1-\lambda} (q_{su} - \omega_k C_b) \tag{2.24}$$

(3) Equations for Particle Distribution

[4] JSCE (1999). *Handbook of hydraulics formulas*. Ver.H12y, pp.167-168. (in Japanese)

[5] Van Rijn, L.C.: Mathematical modelling of suspended sediment in non-uniform flow, Journal of Hydraulic Engineering, ASCE, Vol.110, No.11, 1984.

When bed deformation occurs, particle size distribution in the bed also changes. Therefore, it is necessary to timely calculate the new particle size distribution. According to mass conservation law of bed material, the percentage weight p_{bk} of particle class with diameter d_k can be calculated as follows.

For the bed aggradation ($\frac{\partial Z_b}{\partial t} \geq 0$)

$$\frac{\partial p_{bk}}{\partial t} + \frac{1}{(1-\lambda)E_m}\frac{1}{g_{11}g_{22}}\left[\frac{\partial}{\partial \xi}\left(g_{22}q_{sk\,\xi}\right) + \frac{\partial}{\partial \eta}\left(g_{11}q_{sk\,\eta}\right)\right] + \frac{p_{bk}}{E_m}\frac{\partial Z_b}{\partial t} = 0 \qquad (2.25)$$

For the bed degradation ($\frac{\partial Z_b}{\partial t} < 0$)

$$\frac{\partial p_{bk}}{\partial t} + \frac{1}{(1-\lambda)E_m}\frac{1}{g_{11}g_{22}}\left[\frac{\partial}{\partial \xi}\left(g_{22}q_{sk\,\xi}\right) + \frac{\partial}{\partial \eta}\left(g_{11}q_{sk\,\eta}\right)\right] + \frac{p_{bk0}}{E_m}\frac{\partial Z_b}{\partial t} = 0 \qquad (2.26)$$

where E_m is the thickness of exchange layer, p_{bk0} is the percentage weight of particle class with size d_k in the substratum layer below the exchange layer. The exchange layer is in the surface of river bed and is a concept, where the sediment transports actively. Below the exchange layer, the bed is called as the substratum layer where the sediment transports passively.

2.3 Initial and Boundary Conditions

2.3.1 Initial Conditions for Water Flow

The initial hydraulic conditions are taken as the corresponding boundary values at the beginning. The initial water level is specified according to the observation at the beginning of rainy season. The initial velocity is specified as zero because the reservoir sedimentation simulation starts at the beginning of rainy season and the inflow discharge is almost ignorable.

2.3.2 Boundary Conditions for Water Flow

At the downstream boundary (dam location), discharge of water releasing from spillway and intake (for hydropower plant) is specified. Temporal flow-rate is specified at the upstream boundary of the inflow rivers. The impenetrable condition is applied to the bank boundaries, i.e., the velocity normal to the bank is equal to zero and the tangential component, conforming to the resistance law, is not zero.

2.3.3 Initial Conditions for Sediment Transport

The initial bed elevation and the particle size distribution of bed material are specified according to the measurements. The initial concentration of suspended load is specified as zero because the reservoir sedimentation simulation starts at the beginning of rainy season.

2.3.4 Boundary Conditions for Sediment Transport

Equilibrium bedload transport is assumed at the open boundaries. In this case, suspended load transport dominates in reservoir sedimentation and bedload transport is minor.

In generally, transport of fine sediment, including washload, is independent of local hydraulic conditions and is hardly evaluated directly by general empirical formula. Herein, suspended sediment concentration in inflow is assumed to be a function of the corresponding flow discharge as follows.

$$Q_s = a \cdot Q^b \qquad (2.27)$$

in which Q_s = transport rate of volumetric suspended sediment (m^3/s), Q = discharge (m^3/s) in river, a and b are the parameters. Based on the observed concentration and its particle distribution in inflow, the measured sedimentation in reservoir and sediment release from the reservoir and other related information, the parameter a and b are determined. The particle size distribution of suspended sediment with the inflow is taken into account in the simulation.

The sediment releases together with the water from the reservoir through the Intake for power plant. Because the water is taken near the bed through the Intake, the released concentration of suspended load is specified as that near bed. It is calculated according to the depth-averaged concentration C and the equation (2.23).

2.4 Numerical Method

A "staggered" grid (Figure 2.4.1) arrangement is employed, i.e., components of vectors, e.g., velocity, are "staggered" with scalar variables, e.g., water level, suspended load concentration and bed elevation which are at the center of the control volume. The governing equations for water flow are discretized by a control volume based finite difference scheme and solved first (Jin *et al*, 1997) [6]. Then concentration of suspended sediment is solved, and the bed load transport rate is calculated. Finally bed variation (sedimentation) is evaluated with Eq.(2.24).

Starting from certain initial conditions and under specified boundary conditions, the simulation is carried out step by step and the time varying velocity fields, water surface level, sediment transport rate and sedimentation (bed level variation) are evaluated.

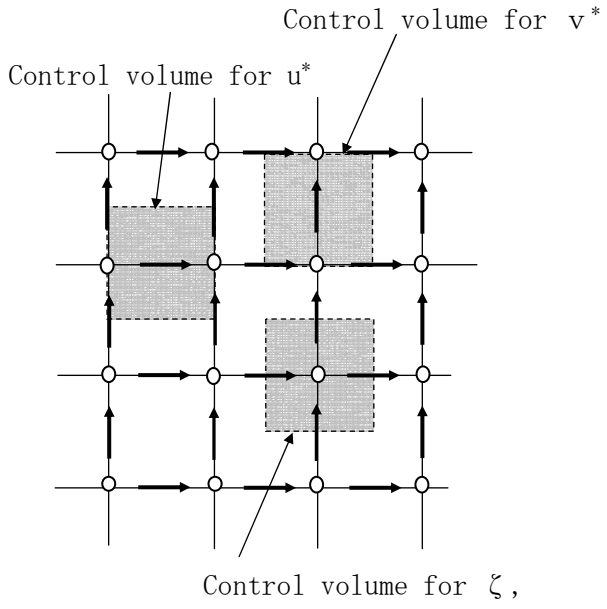

Figure 2.4.1 'Staggered' Grid

[6] Jin, H.S., Egashira, S.,and Liu, B.Y. (1997). 3-D Numerical Solution of Flow in Sine-generated Meandering Compound Channel. *Proceedings of 27th IAHR Congress*, San Francisco, USA. pp.246-251.

CHAPTER 3 CALIBRATION OF THE SEDIMENTATION MODEL IN WONOGIRI RESERVOIR

In this project, the above reservoir sedimentation analysis model, NKhydro2D model, has been applied to the Wonogiri multipurpose reservoir in the Republic of Indonesia. The surface area of the reservoir is about 88km^2 and the maximum depth is about 18m at the control water level. The initial storage capacity of the reservoir was about 7.3×10^8 m^3. The sedimentation volume during the past 25 years has reached to about 1×10^8 m^3 and the situation is deteriorating.

First, based on the observed flow discharge and concentration of suspended load in the inflowing rivers, water and sediment release through the Intake and spillway, and the measured sedimentation during the rainy season of 2004-2005, the sediment into the reservoir from the inflowing rivers during the season, which was supplied from the upland area, is evaluated by the equation (2.27).

Then, the sedimentation analysis model is calibrated and verified by the field data surveyed during rainy season of 2004-2005 as well those during 1993-2004. The computational results on the sedimentation and particle size distribution in the reservoir, the volume and its concentration of sediment release through the Intake for power plant, and the water surface level during the season are compared with the measurements. There is good agreement between the computation and the measurement.

The result shows that the equation (2.27) for the inflowing rivers is reasonable and the NKhydro2D model can be applied to evaluate the sedimentation in the Wonogiri reservoir.

3.1 Computational Domain and Grids

Because of complicated plan-form of the reservoir, which includes 6 major inflow rivers (Bengawan Solo River and its tributaries), the model is based on a boundary-fitted numerically generated orthogonal curvilinear coordinate system. The domain of interest, which covers the reservoir and 6 major inflow rivers (Bengawan Solo River, Keduang River, Tirtomoyo River, Temon River, Alang River and Wuryantoro River), and the numerically generated boundary-fitted orthogonal curvilinear grids are shown in Figure 3.1.1. The upstream ends of the inflow river are located at where effect due to backwater from the Wonogiri reservoir could almost be ignored.

The total grids are about 3,700 and the grid size is about 3 m-330 m for the effective and accurate simulation. The grids are set to be finer in area of the inflow river and near the Wonogiri multipurpose dam, while coarser grids are set in center of the reservoir.

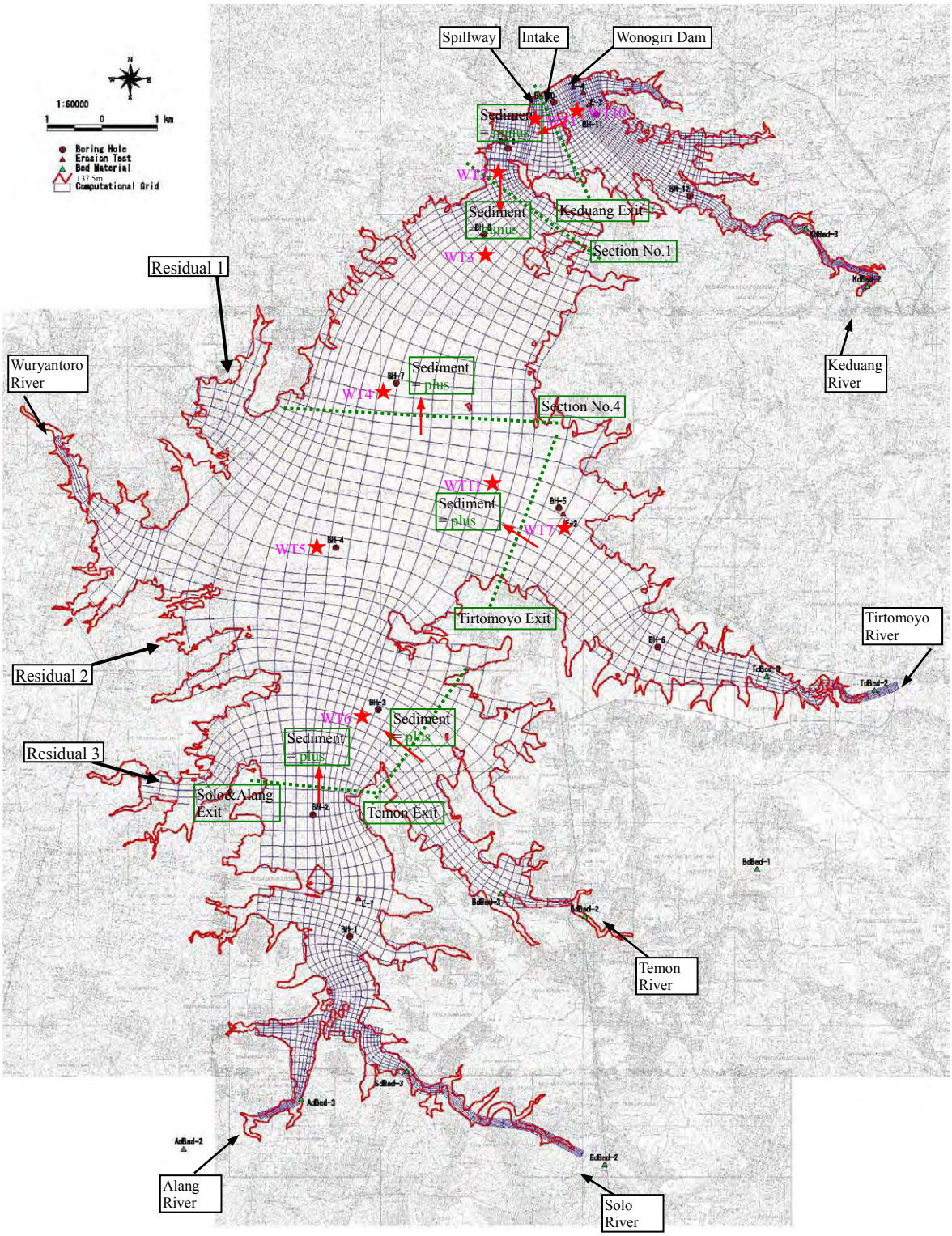

Figure 3.1.1 Wonogiri Reservoir and its Contour of 137.5 m, Location of Boring Hole (BH), Bed Material Sampling (Bd) and Water Quality Survey (WT), and the Computational Mesh

3.2 Sedimentation Volume in the Reservoir during Rainy Season of 2004-2005

Topographic and bathymetric surveys (mainly echo sounding surveys) were conducted in October 2004 and July 2005, respectively. The rainy season of 2004-2005 started from November 2004 and ended in May 2005. Out of the rainy season, sediment inflow can be ignored because the water inflow is minor and the corresponding concentration of suspended sediment (SS) is very lower.

By comparing the variation of bed elevation between October 2004 and July 2005, the sedimentation volume during the season can be estimated (Table 3.2.1). The divisions of area are shown in Figure 3.2.1. The Keduang area in Table 3.2.1 consists of Keduang area and Dam area in Figure 3.2.1.

It is understood that this sedimentation was resulted from the balance between the sediment supply from the rivers (evaluated by equation (2.27)) and the sediment release through the Intake and the spillway.

Table 3.2.1 Sedimentation Volume in Wonogiri Reservoir during 2004-2005 (m^3, including Void)

Area	Sedimentation Volume (m3)	Sediment Distribution(%)								
		d= 0.0013mm	0.0013– 0.005mm	0.005– 0.016mm	0.016– 0.031mm	0.031– 0.075mm	0.075– 0.25mm	0.25– 0.85mm	0.85– 2.0mm	2.0– 19.0mm
Keduang	711,500	58.01	6.22	8.97	7.00	8.77	9.22	1.69	0.12	0.00
Tirtomoyo	304,500	51.74	3.20	5.20	3.92	6.35	10.82	14.22	4.18	0.38
Temon	98,600	61.33	5.97	10.17	6.20	9.41	6.33	0.37	0.21	0.00
Solo&Alang	400,300	63.47	4.49	10.65	7.86	8.52	4.04	0.74	0.23	0.00
CenterUP+ Wuryantoro3	471,800	56.43	4.23	9.03	5.45	8.39	10.51	4.39	1.33	0.24
Center	208,300	79.75	3.47	3.49	1.77	3.32	4.45	2.08	1.40	0.28
Wuryantoro	96,000	unknown								
Wuryantoro2	25,800	unknown								
Total	2,316,800									

Table 3.2.1 shows that sedimentation volume in the reservoir during 2004-2005 was about 2,317,000m^3 (deposition volume, including void. The following volumes are all in deposition base). Herein, dry density of bed material in the Wonogiri reservoir is 1,064kg/m^3 and density of soil particle is 2,650kg/m^3.

Area-averaged size distributions of deposited bed material, calculated according to boring tests in October 2004 (please refer to Figure 3.1.1 for the locations), are also listed in Table 3.2.1. The size distributions of bed material at the boring locations are shown in Table 3.2.2 and Figure 3.2.2. According to Table 3.2.1 and Figure 3.2.2, it is understood that the sediment in center of the reservoir is quite fine.

In simulation, the sediment is divided into 9 classes, as shown in Table 3.2.3. The initial distribution of bed material as the initial condition of simulation is set according to these boring data.

Table 3.2.2 Particle Size Distribution of Bed Material at Boring Locations (%, October 2004)

Diameter (mm)	88.9000	74.6449	50.8000	38.1000	19.1000	9.5000	2.0000	0.8500	0.2500	0.0750	0.0310	0.0160	0.0050	0.0013
BH1			100.00	100.00	100.00	100.00	100.00	99.53	98.53	94.77	85.83	75.99	66.80	63.51
BH2			100.00	100.00	100.00	100.00	100.00	99.99	99.13	97.11	89.90	82.37	69.78	65.57
BH3			100.00	100.00	100.00	100.00	100.00	99.79	99.42	93.08	83.67	77.47	67.30	61.33
BH4			100.00	100.00	100.00	100.00	99.29	95.51	83.58	60.40	51.87	49.24	44.90	42.38
BH5			100.00	100.00	100.00	100.00	99.83	98.55	92.27	80.32	75.19	71.73	65.36	61.22
BH6			100.00	100.00	100.00	100.00	99.33	89.48	55.16	39.11	28.51	21.97	16.24	14.24
BH7			100.00	100.00	100.00	100.00	99.72	98.32	96.24	91.79	88.48	86.71	83.22	79.75
BH8			100.00	100.00	100.00	100.00	100.00	99.85	99.32	97.76	93.28	91.12	87.68	84.19
BH9			100.00	100.00	100.00	100.00	100.00	99.88	99.59	98.97	95.79	90.45	81.93	77.17
BH10			100.00	100.00	100.00	100.00	100.00	99.95	94.88	67.17	53.44	45.30	35.01	28.82
BH11			100.00	100.00	100.00	100.00	100.00	99.90	99.79	99.28	88.78	76.49	63.01	52.81
BH12			100.00	100.00	100.00	100.00	100.00	99.81	97.38	81.66	69.69	62.62	53.51	47.04
KdBed-2	100.00	100.00	92.78	83.04	48.89	31.78	15.04	9.49	3.33	1.80	1.58	1.43	1.25	1.15
KdBed-3	100.00	96.77	83.43	70.47	33.59	20.05	11.66	9.57	5.55	2.72	1.82	1.58	1.23	0.97
TdBed-2(1	100.00	100.00	100.00	100.00	100.00	99.62	98.92	90.13	50.63	25.47	17.39	13.94	9.32	7.98
TdBed-2(2	100.00	97.53	94.04	88.68	67.24	48.15	27.03	21.29	10.71	4.70	2.95	2.68	2.37	2.20
TdBed-3	100.00	100.00	100.00	100.00	100.00	100.00	91.52	69.78	34.59	18.14	11.47	9.59	7.47	6.60
BdBed-2	100.00	100.00	98.80	96.80	84.56	60.81	21.72	15.38	7.32	4.53	2.83	2.48	2.04	1.72
BdBed-3	100.00	100.00	100.00	100.00	100.00	100.00	100.00	77.31	43.22	32.57	27.13	24.55	20.64	18.08
SdBed-2	100.00	96.96	87.13	80.53	48.19	36.05	26.25	18.91	8.68	4.62	2.86	2.60	2.11	1.94
SdBed-3	100.00	100.00	100.00	100.00	98.76	96.64	91.39	70.61	35.45	14.61	9.94	9.02	7.28	6.70
AdBed-3	100.00	100.00	100.00	100.00	100.00	99.43	94.67	87.28	47.32	25.74	21.12	19.23	15.52	12.39

Table 3.2.3 Particle Size Division (9 Classes) of Bed Material for Simulation

Diameter Range of Class (mm)	~0.0013	0.0013 ~0.005	0.005~ 0.016	0.016~ 0.031	0.031~ 0.075	0.075 ~0.25	0.25~ 0.85	0.85~ 2.0	2.0~ 19.0
Mean Diameter of Class (mm)	0.0013	0.0026	0.0089	0.0223	0.0482	0.137	0.461	1.304	6.164

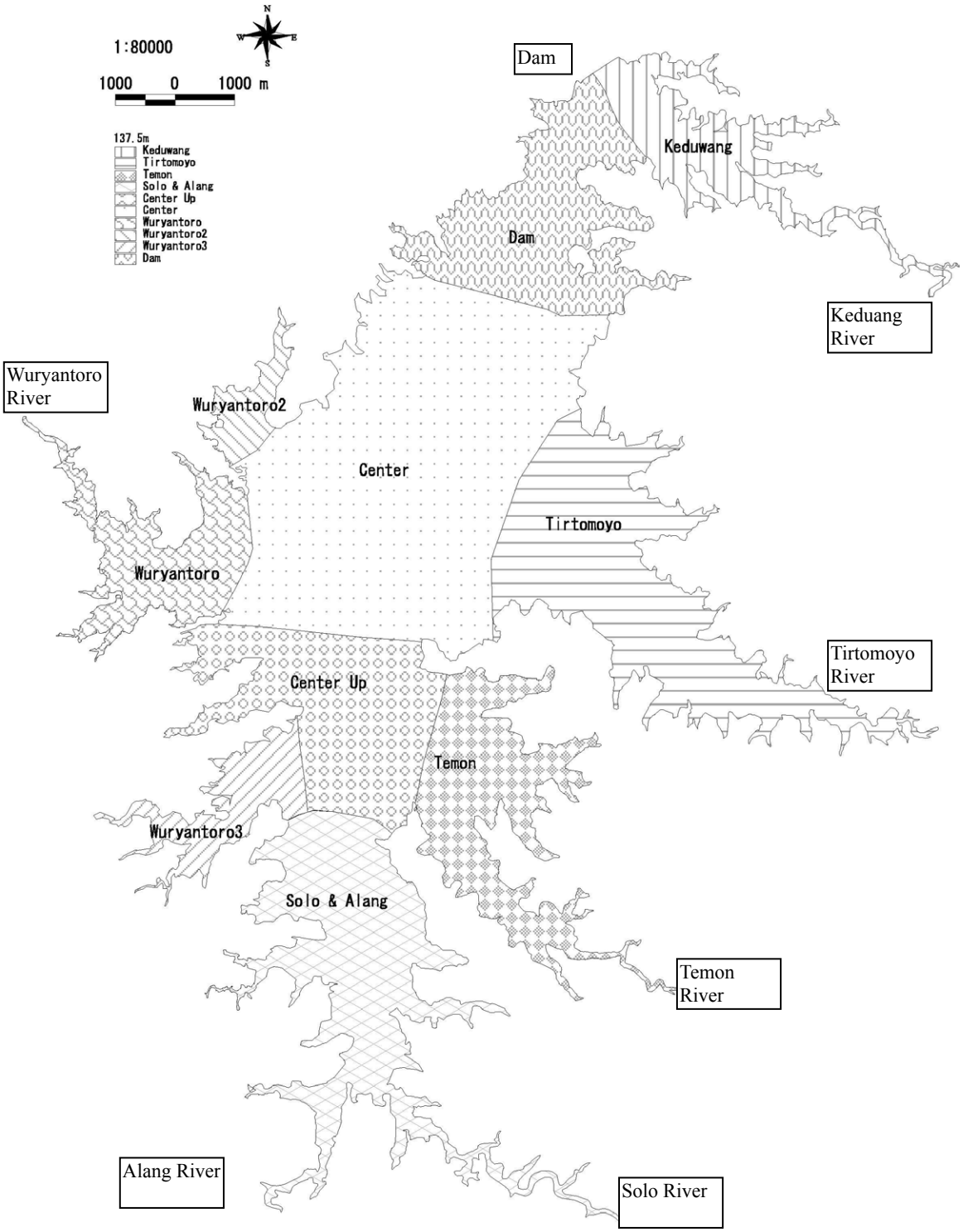

Figure 3.2.1 Sub-territory Division for Calculating the Sedimentation in the Wonogiri Reservoir

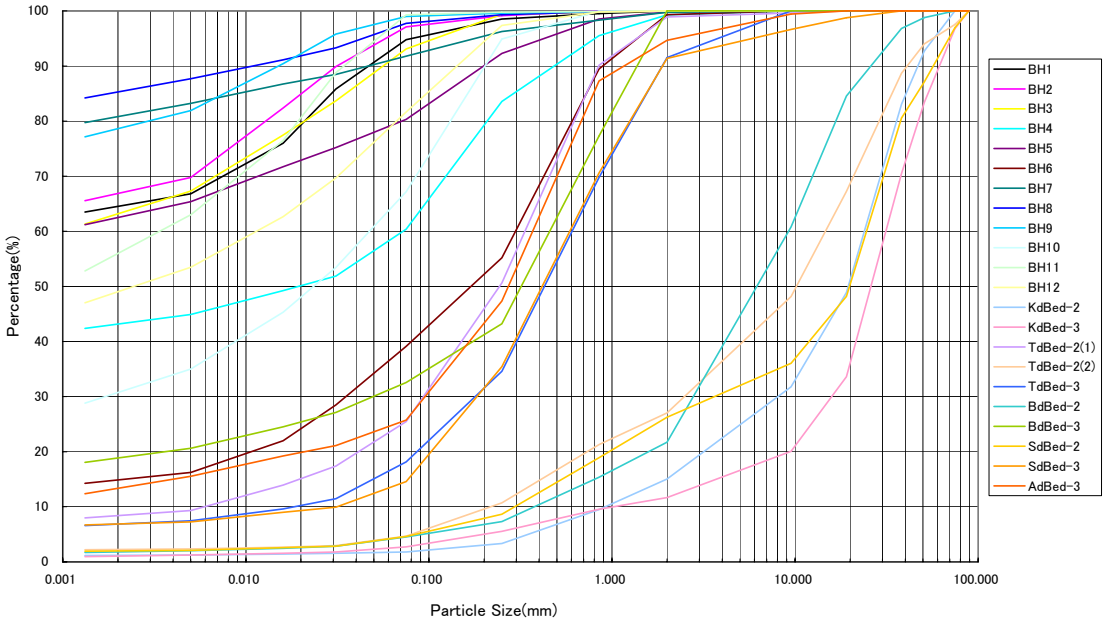

Figure 3.2.2 Particle Size Distribution of Bed Material at Boring Locations (October 2004)

3.3 Estimation of Inflowing Sediment to the Wonogiri Reservoir

Besides the topographic surveys, inflowing discharge in the rivers during November 23, 2004 ~ May 15, 2005 was also observed. Water samples were also taken for analyzing the concentration and its particle size distribution of suspended load during flood of the season.

Discharge hydrographs of inflow from the main rivers and the residual basin are shown in Figure 3.3.1~3.3.6. Figure 3.3.7 shows hydrograph of the total inflow. During the rainy season of 2004-2005, maximum flood occurred on 3 December 2004 and the peak discharge of total inflow was about 1,330 m^3/s. Much more floods occurred in Keduang River.

Water release through the intake is shown in Figure 3.3.8. During the rainy season of 2004-2005, water release through the spillway was almost zero because the season was a hydrological drought year.

Based on these measurements and the records of water and sediment release, inflowing sediment as well as the parameters, a and b, in equation (2.27) for each river can be estimated.

Test simulation by NKhydro2D model and site investigation show that an absolute majority of sediment inflow to the reservoir is suspended sediment (including washload). Here, bed load is ignored in the estimation of sediment inflow volume because of its absolute minority in the total. Therefore, the sedimentation volume in table 3.2.1 is taken as contribution of suspended sediment (including washload) from the rivers.

3.3.1 Sediment Release from the Reservoir in the Rainy Season of 2004-2005

Together with the water release, part of the sediment inflow was released out of the reservoir by the spillway and the intake. Its volume can be estimated by the outflow discharge of water and the concentration of SS near the facilities. There was no sediment

release from the spillway during the rainy season of 2004-2005 because the spillway was not run. It is possible to estimate the sediment outflow by the intake discharge of hydropower plant and its SS concentration.

Turbidity in the intake of hydropower plant had been observed during January ~ May, 2005, and sampling analyses at WT1 near the intake (Figure 3.1.1) were conducted for its SS concentration. Figure 3.3.9 shows the relationship between SS and Turbidity at WT1 and the following equation (3.1) can be obtained.

$$SS = 1.342 \cdot Turbidity \qquad (3.1)$$

where SS = concentration of SS in ppm, $Turbidity$ = the corresponding turbidity in NTU.

Based on the observed turbidity and discharge (Figure 3.3.8) in the intake and the equation (3.1), the sediment release by the intake from January 5 to May 15, 2005 was estimated to be about 71,300m^3 and its average SS concentration was 554.2ppm. Furthermore, the sediment release by the intake from November 23, 2004 to January 4, 2005, can be estimated to be about 54,800m^3, if the average SS concentration from January to May 2005 is applied to that in the period. Therefore, the sediment outflow from November 23, 2004 to May 15, 2005 was about 126,100m^3. Observation of flood discharge in the rivers had been conducted during November 23, 2004 ~ May 15, 2005, and the reservoir sedimentation is also simulated in this period.

In addition, the sediment outflow from May 16 to the end of June 2005 was eltimated to be about 7,500m^3. It is known that discharge water from the hydropower plant of the reservoir is clear in dry season. Therefore, it can be estimated that the total sediment outflow from October 2004 to July 2005 (the measurement interval of reservoir topography) was about 135,000m^3.

3.3.2 Sediment Inflow from Each River in the Rainy Season of 2004-2005

According to the sedimentation volume in Table 3.2.1 and this sediment release volume, the total sediment inflow was estimated to be about 2,452,000m^3 in the period of October 2004 to July 2005.

This total volume of sediment inflow is then allocated to the rivers according to the flood observation and SS sampling analysis (its concentration and particle size distribution), sedimentation and its size distribution in division area and sediment outflow, as well as test simulation by NKhydro2D model, as shown in Table 3.3.1.

Table 3.3.1 Sediment Inflow Volume from the Rivers during the Period of 2004.10~2005.7

Rivers	Basin Area (km^2)	Sediment Inflow (2004.10～2005.7) (deposition volume、m^3)
Keduang	421	825,000
Tirtomoyo	231	420,000
Temon	63	85,000
Solo	206	525,000
Alang	169	346,000
Residual	152	251,000
Total	1,242	2,452,000

3.3.3 Parameters a and b in Equation (2.27) for Each River

With the sediment inflow in the rivers (Table 3.3.1) and the flood observation as well as the SS sampling analysis, the parameter a and b in equation (2.27) for each river can be determined.

Observed flood discharge and sediment (SS) transport rate in Keduang river, Tirtomoyo river, Temon river, Bengawan Solo river and Alang river are plotted in Figure 3.3.10~3.3.14, respectively. With these correlation data, the parameter b in equation (2.27) for each river is first specified as the inclination of the correlation curve, as listed in Table 3.3.2. The parameter for the river in left side of the reservoir is referred to that in Alang river because there was no observation in the area.

Furthermore, parameter a is determined according to the sediment inflow (Table 3.3.2) and water hydrograph in rivers, as listed in Table 3.3.1. The correlation curves are also plotted in Figure 3.3.10~3.3.14. It shows that the estimated correlation curves with parameter a and b fit to the observations. Therefore, the sediment inflows in the rivers during the period of November 23, 2004 ~ May 15, 2005 are estimated as those in Table 3.3.2. The total sediment inflow in the period was 2,390,000m^3 which is a little bit less than that in the period of 2004.10~2005.7 (the difference = 60,000 m^3).

In the simulation, sediment inflow for the sediment with size d_k is specified according to equation (2.27) and the particle size distribution of SS (Table 3.3.3 and Figure 3.3.15) in the rivers.

Table 3.3.2 Parameters of SS ~ Flow Discharge Function and Sediment Inflow in the Rivers

River	a	b	Sediment Inflow during 2004.11.23-2005.5.15 (deposition volume, m^3)
Keduang	0.0002656	1.601	811,000
Tirtomoyo	0.0003967	1.477	409,000
Temon	0.0005219	1.522	85,000
Solo	0.0010536	1.388	506,000
Alang	0.0003738	1.628	335,000
Wuryantoro	0.0004875	1.628	246,000
Total			2,390,000

Table 3.3.3 Particle Size Distribution of the Sediment Inflow in the Rivers (2004.11~2005.5)

River	Sediment Distribution (%)								
	d= 0.0013mm	0.0013- 0.005mm	0.005- 0.016mm	0.016- 0.031mm	0.031- 0.075mm	0.075- 0.25mm	0.25- 0.85mm	0.85- 2.0mm	2.0- 19.0mm
Keduang	65.01	6.22	8.97	7.00	5.77	5.22	1.69	0.12	0.00
Tirtomoyo	57.74	7.20	7.20	6.92	6.35	6.82	5.23	2.18	0.36
Temon	49.33	5.98	11.17	10.20	13.41	8.33	1.37	0.21	0.00
Solo	57.36	4.88	16.22	9.81	8.27	2.42	0.92	0.12	0.00
Alang	63.71	7.80	11.79	7.24	5.79	2.65	0.90	0.12	0.00
Wuryantoro	56.17	4.81	6.63	5.63	7.79	10.23	6.50	1.90	0.34

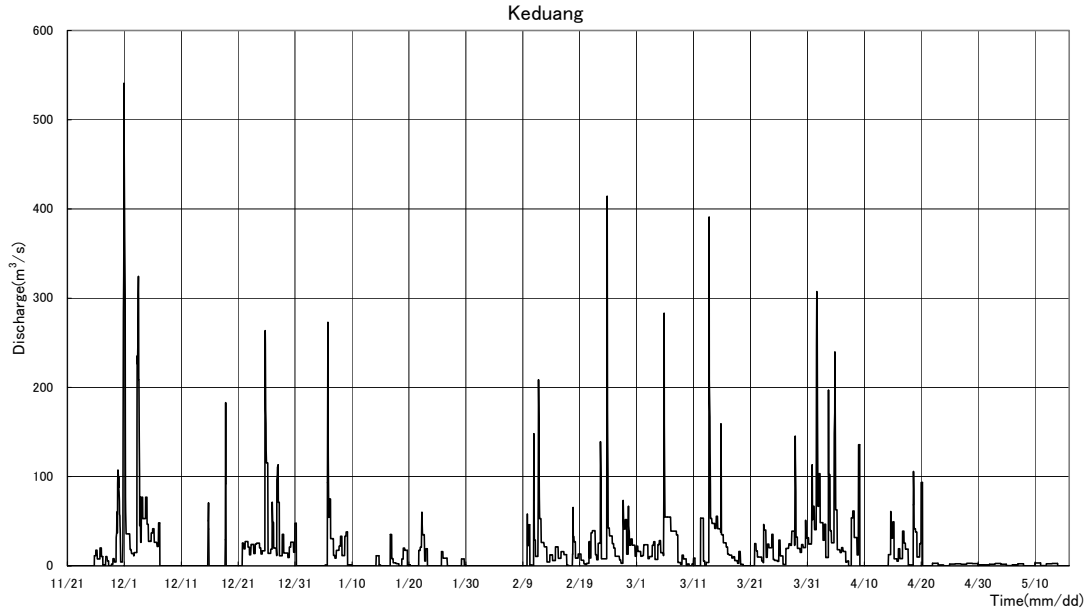

Figure 3.3.1 Hydrograph of Inflow from the Keduang River during November 2004 - May 2005

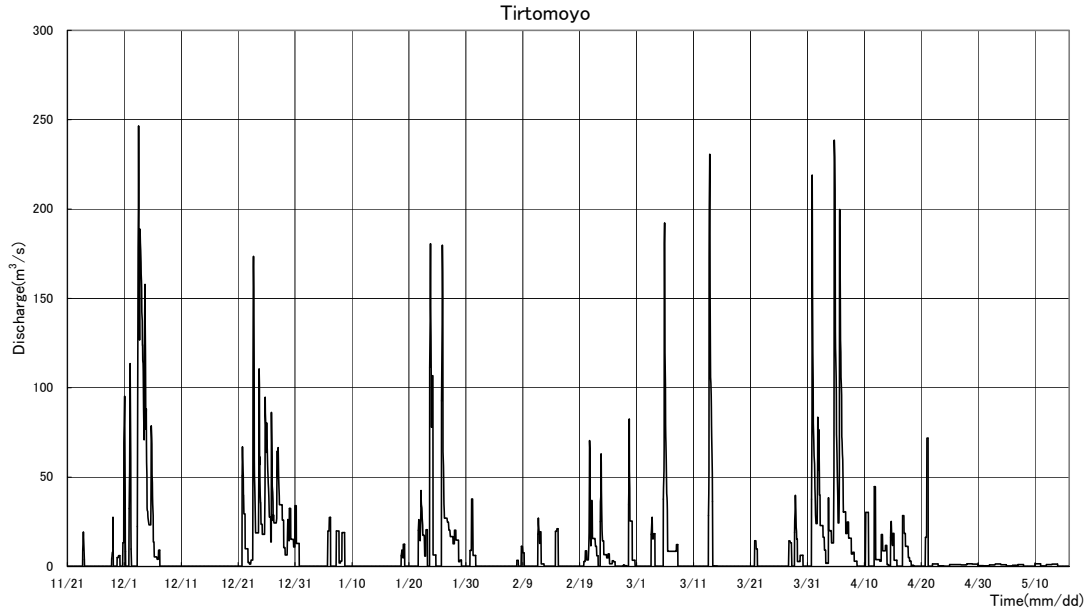

Figure 3.3.2 Hydrograph of Inflow from the Tirtomoyo River during November 2004 - May 2005

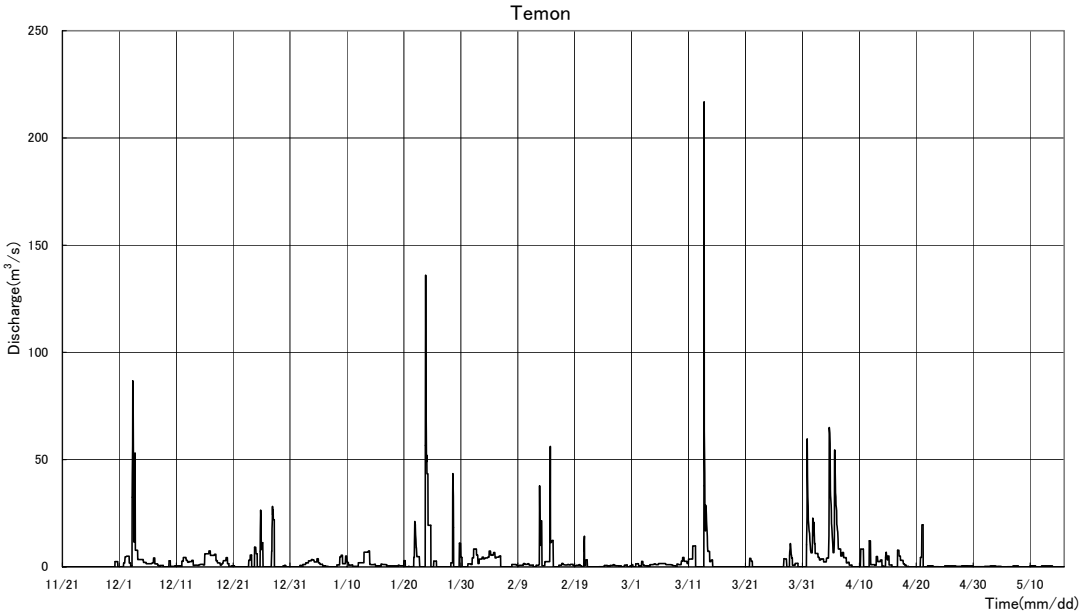

Figure 3.3.3 Hydrograph of Inflow from the Temon River during November 2004 - May 2005

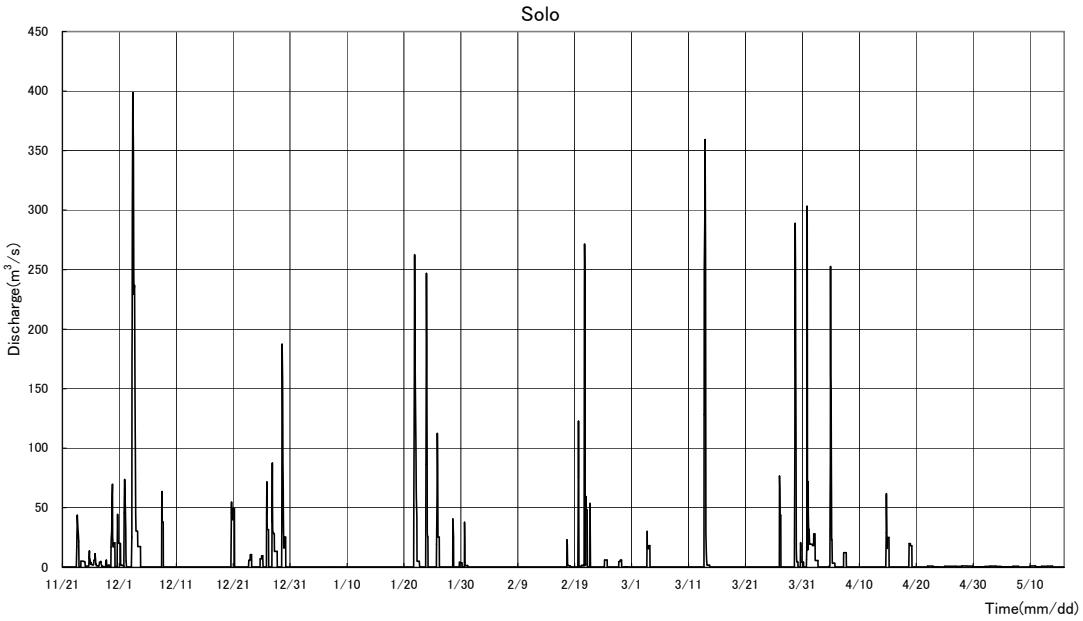

Figure 3.3.4 Hydrograph of Inflow from the Bengawan Solo River during November 2004 - May 2005

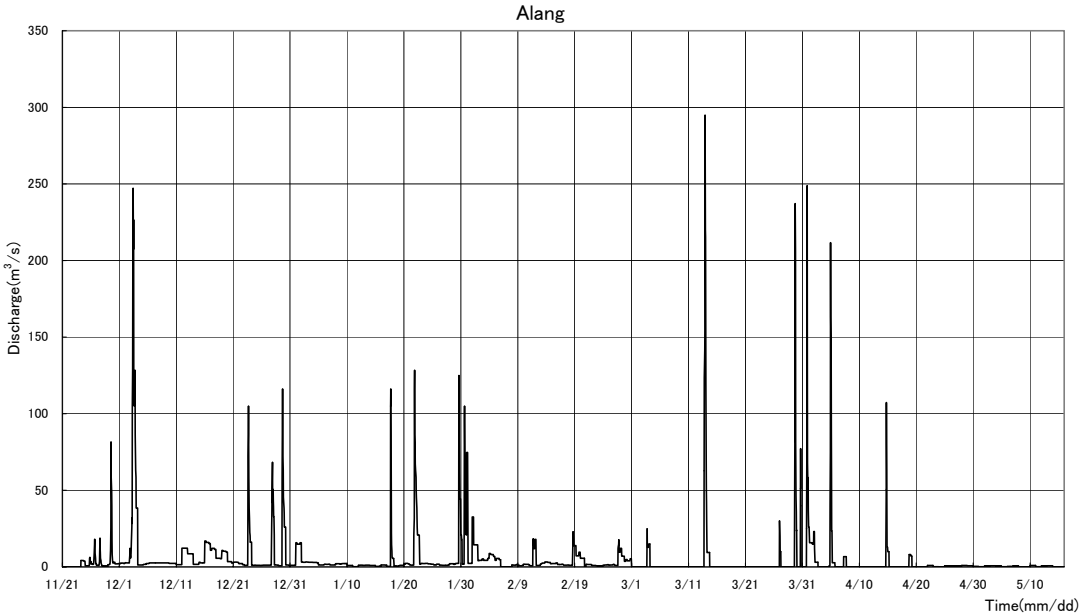

Figure 3.3.5 Hydrograph of Inflow from the Alang River during November 2004 - May 2005

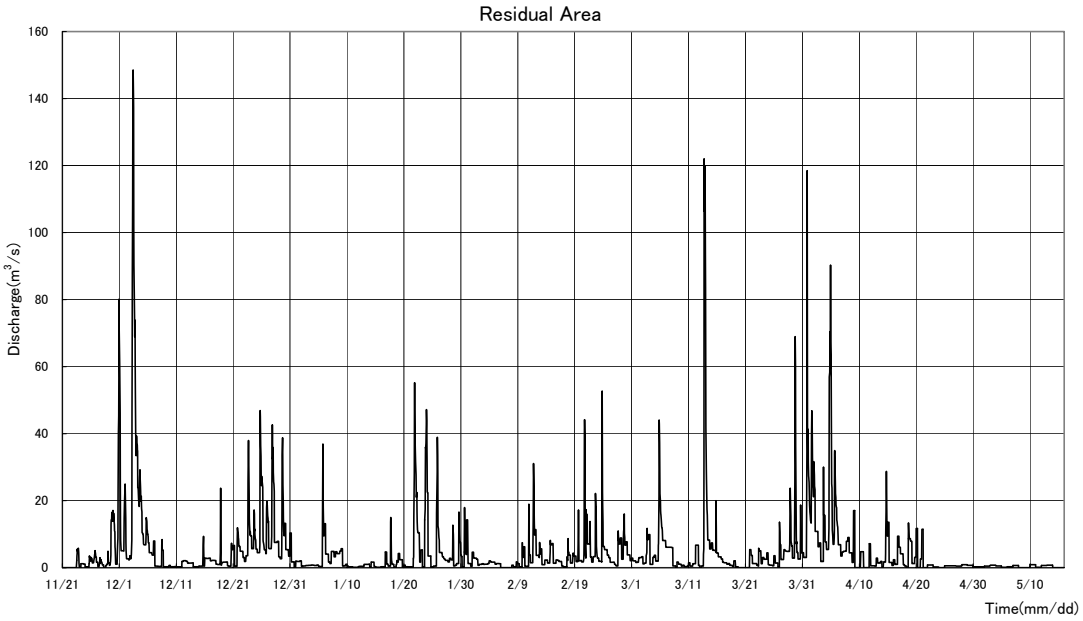

Figure 3.3.6 Hydrograph of Inflow from the Residual Basin during November 2004 - May 2005

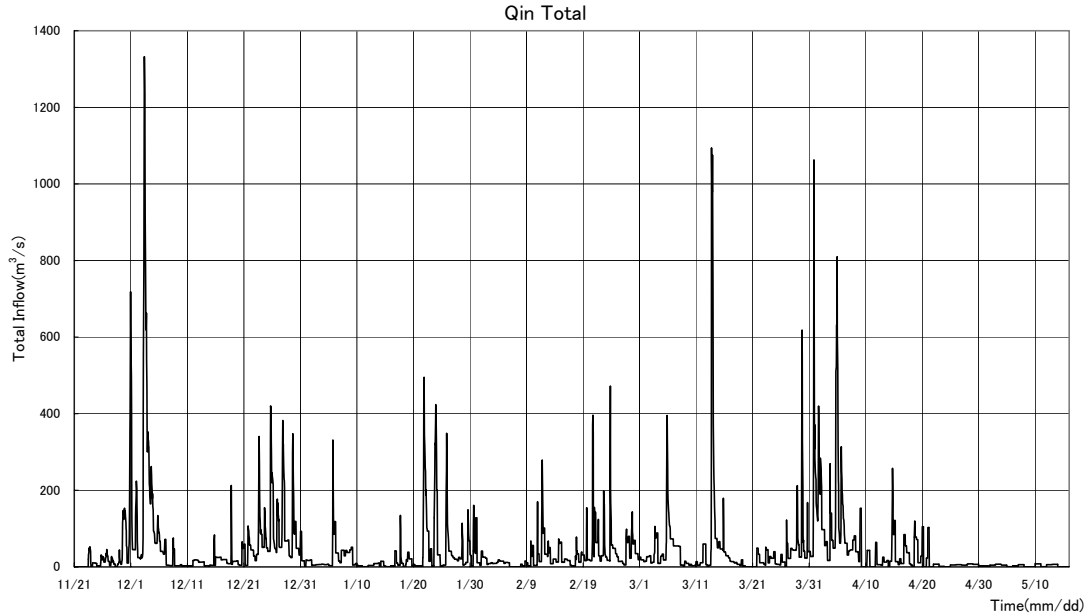

Figure 3.3.7 Hydrograph of Total Inflow during November 2004 - May 2005

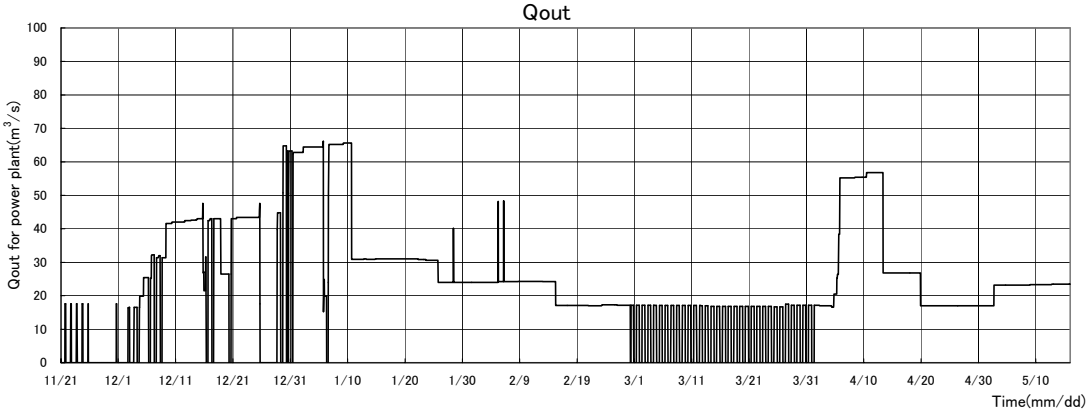

Figure 3.3.8 Water Release through the Intake during November 2004 - May 2005

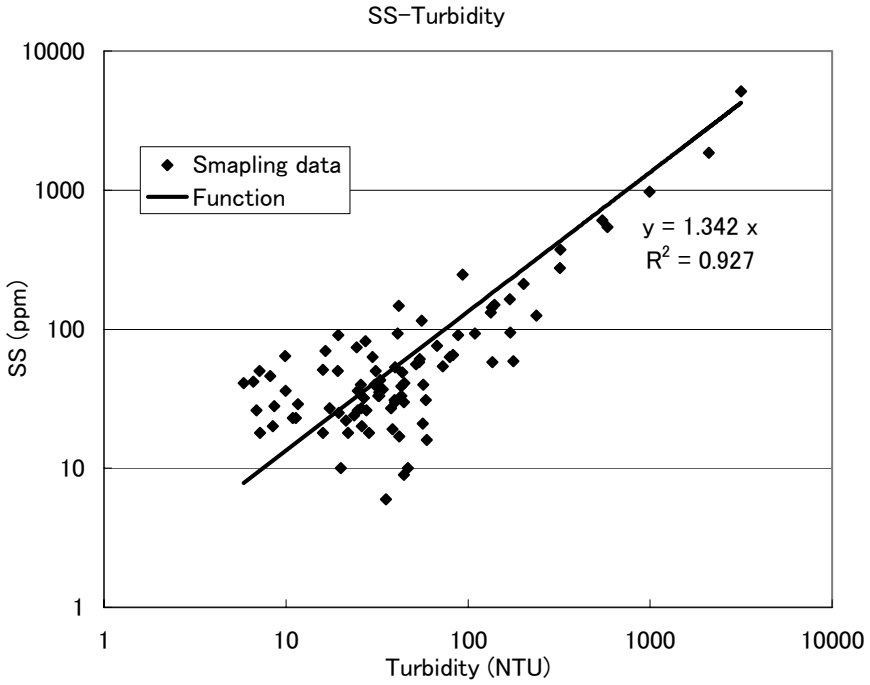

Figure 3.3.9 SS ~ Turbidity Correlation Function at WT1 near the Intake of the Reservoir

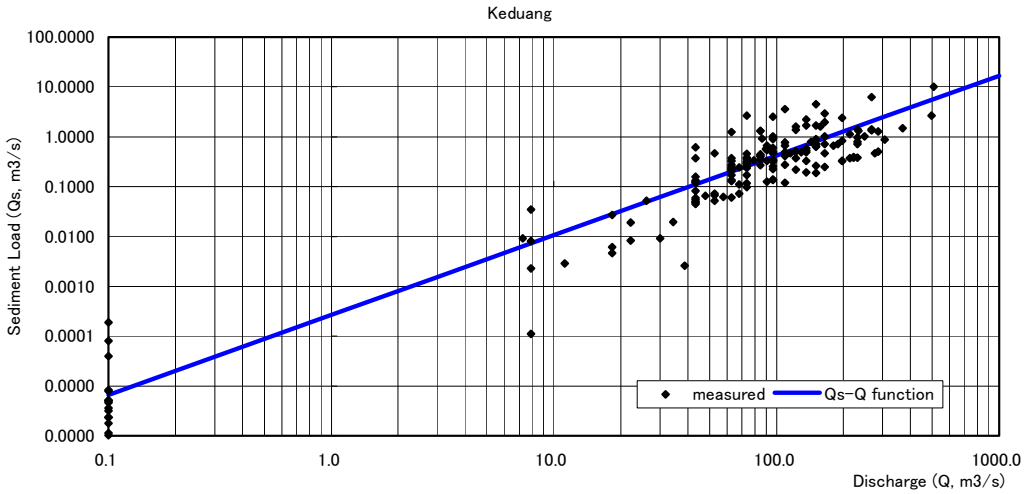

Figure 3.3.10 Observation and Correlation Function of Sediment Transport Rate Q_s ~Water Discharge in Keduang Rivers (2004.11~2005.5)

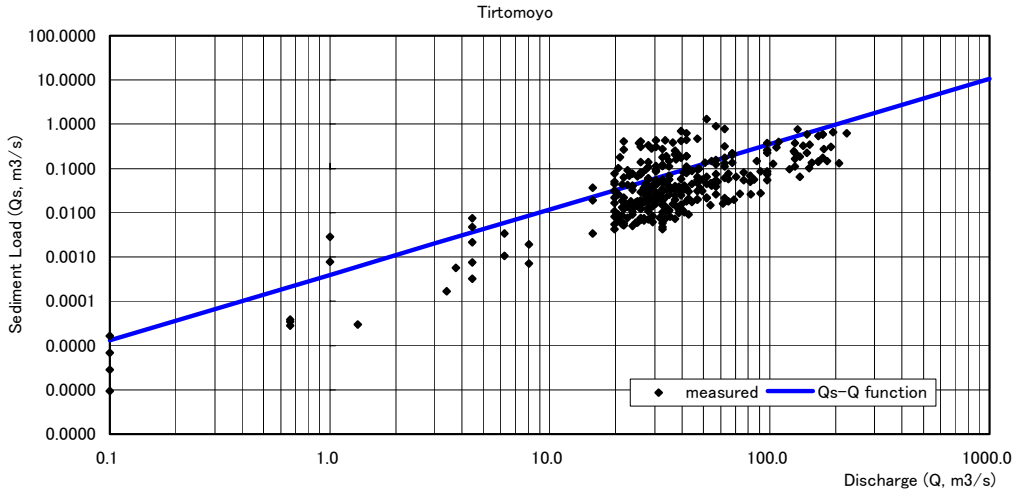

Figure 3.3.11 Observation and Correlation Function of Sediment Transport Rate Q_s ~Water Discharge in Tirtomoyo Rivers (2004.11~2005.5)

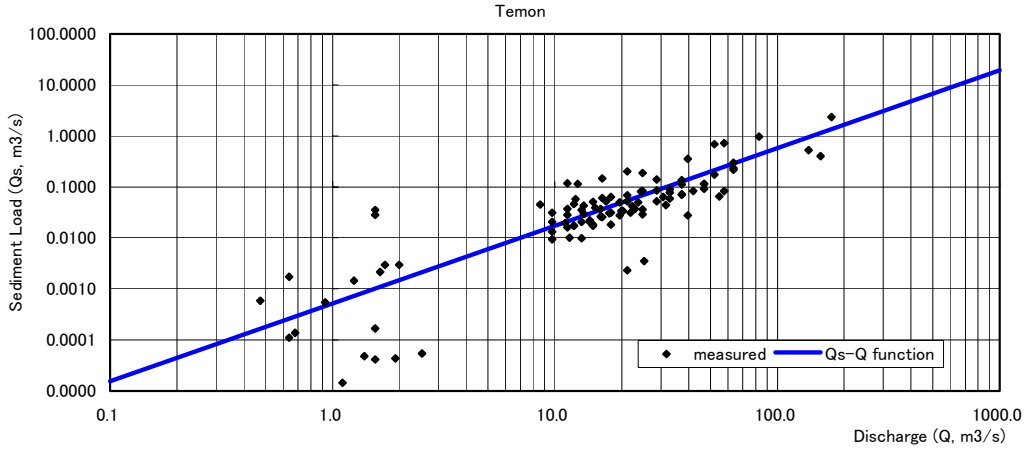

Figure 3.3.12 Observation and Correlation Function of Sediment Transport Rate Q_s ~Water Discharge in Temon Rivers (2004.11~2005.5)

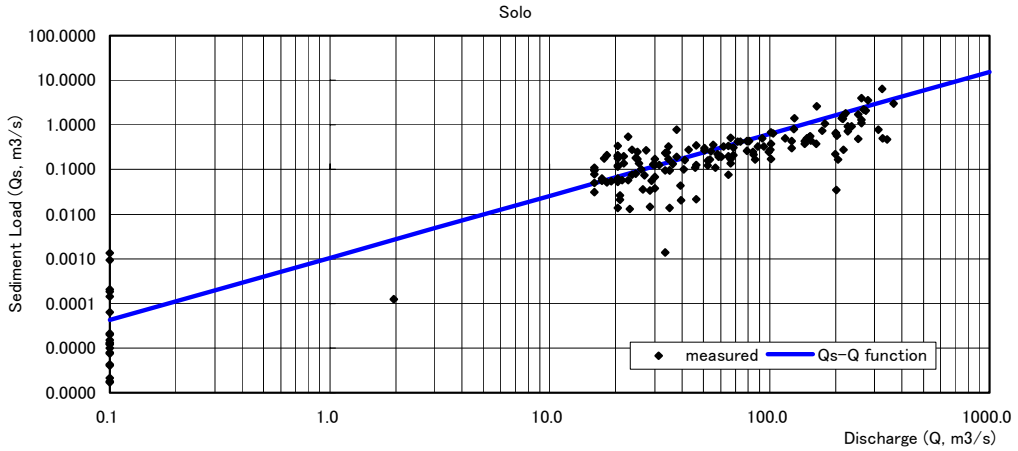

Figure 3.3.13 Observation and Correlation Function of Sediment Transport Rate Q_s ~Water Discharge in Bengawan Solo Rivers (2004.11~2005.5)

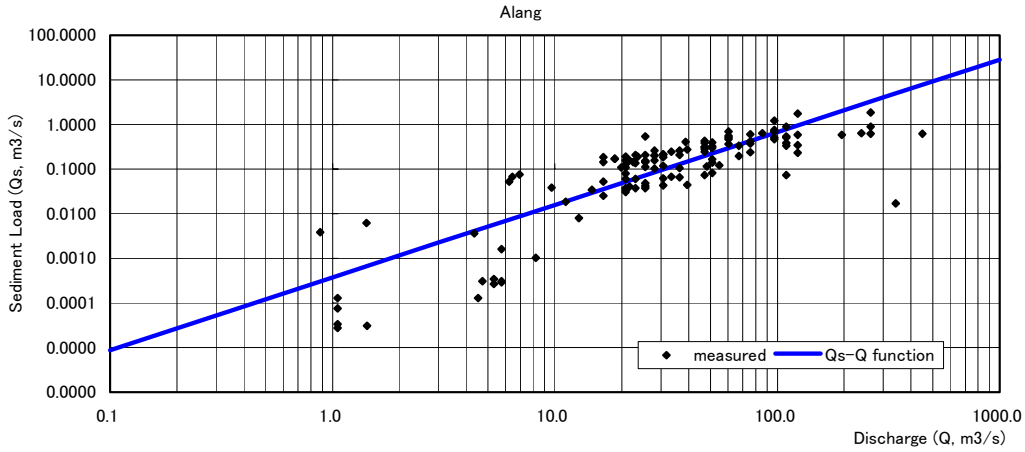

Figure 3.3.14 Observation and Correlation Function of Sediment Transport Rate Q_s ~Water Discharge in Alang Rivers (2004.11~2005.5)

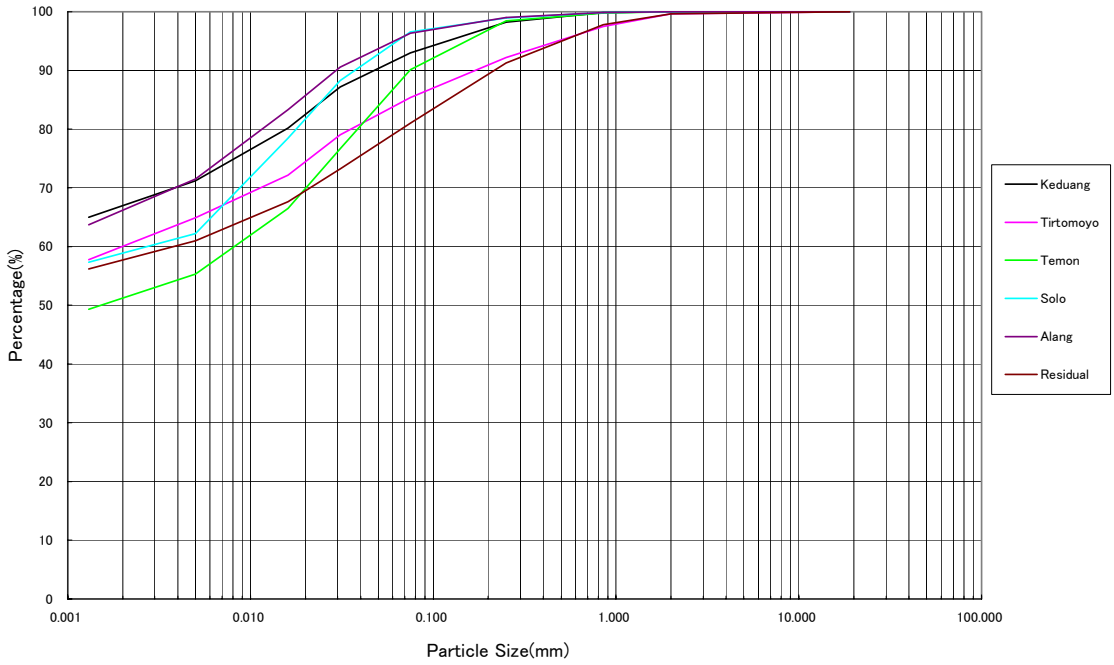

Figure 3.3.15 Particle Size Distribution of Sediment Inflow in the Rivers (2004.11~2005.5)

3.4 Calibration of Reservoir Sedimentation Analysis Model by the Measurements in the Rainy Season of 2004-2005

By the specification of sediment inflow equation (2.27) and discharge hydrograph in the rivers, the afore-mentioned model, NKhydro2D model, is applied to analyze the sedimentation in the Wonogiri reservoir. Firstly, the model is calibrated by the field data surveyed during rainy season of 2004-2005. Then the model is verified by the survey data during 1993-2004.

3.4.1 Initial and Boundary Conditions

Besides the information of computational mesh, other input conditions for the sediment transport model, including the inflow discharge and sediment supply, are necessary as initial and boundary conditions. The input conditions for simulation during the rainy season of 2004-2005 are listed in Table 3.4.1.

Table 3.4.1 Input Data for Simulation during the Rainy Season of 2004-2005

Item	Data	Note
Methodology	Depth-integrated 2-dimensional sediment transport model—NKhydro2D model	Based on boundary-fitted orthogonal curvilinear grids
Topogrphical Map	Topographical map with the scale 1:25,000	Published in 1999
Bathymetric data	Cross-section data measured in October 2004	
Inflow Discharge	Temporal discharge (hourly) is employed.	Peak discharge of total inflow is about 1,330m^3/s occurred on December 3, 2004
Water Release	Records of both the spillway and the intake	Almost no water release through the spillway during this season
Water Level	The initial water level is specified as the measured reservoir water level at the starting of simulation.	Started at 0:00, Nov.21, 2004 The initial velocity is set to zero.
Bed Material	Data of particle size distribution at different locations sampled in October 2004. As non-uniform material (consists of 9 classes in simulation)	The size in deeper area is quite fine.
Sediment Transport Mode	As both the bed load and suspended load	Non-uniform sediment (consists of 9 classes in the simulation)
Sediment Supply	Sediment transport rate for bed load is calculated by Ashida & Michiue's formula. Concentration of suspended sediment is specified as function of river discharge.	Particle size distribution is considered.
Sediment Release	Sediment release accompanied with water release through the spillway and intake is considered.	Bottom concentration of suspended sediment is specified as the release concentration from the intake.
Other Information	Rainfall, Evaporation, etc.	

(1) Initial Bed Level and Particle Size Distribution of Bed Material

Figure 3.4.1 shows the contour of bed level, measured in October 2004, in the Wonogiri reservoir. This is specified as the initial bed level for the simulation during the rainy season of 2004-2005.

As shown in Figure 3.4.1, sedimentation in Wonogiri reservoir was very severe. Among the others, maximum depth of sedimentation in Keduang River area had reached about 20m and that near the intake was over 10m, while that in center of the reservoir was about 1m. In Tirtomoyo River and Temon River area, sedimentation depth was about 5m. In upstream part of the reservoir, Bengawan Solo River and Alang River area, sedimentation depth was about 3-7m.

Figure 3.4.2 shows the measured H-A (water level ~ surface area) and H-V (water level ~ capacity volume) curves in October 2004. For the comparison, the calculated H-A and H-V curves by the initial bed level in simulation are also shown in Figure 3.4.2. It is understood that the setting of initial bed in simulation is consistent with the measurement.

In simulation, the sediment is divided into 9 classes, as shown in Table 3.2.3. The initial particle size distribution of bed material is specified according to the boring data (Table 3.2.2).

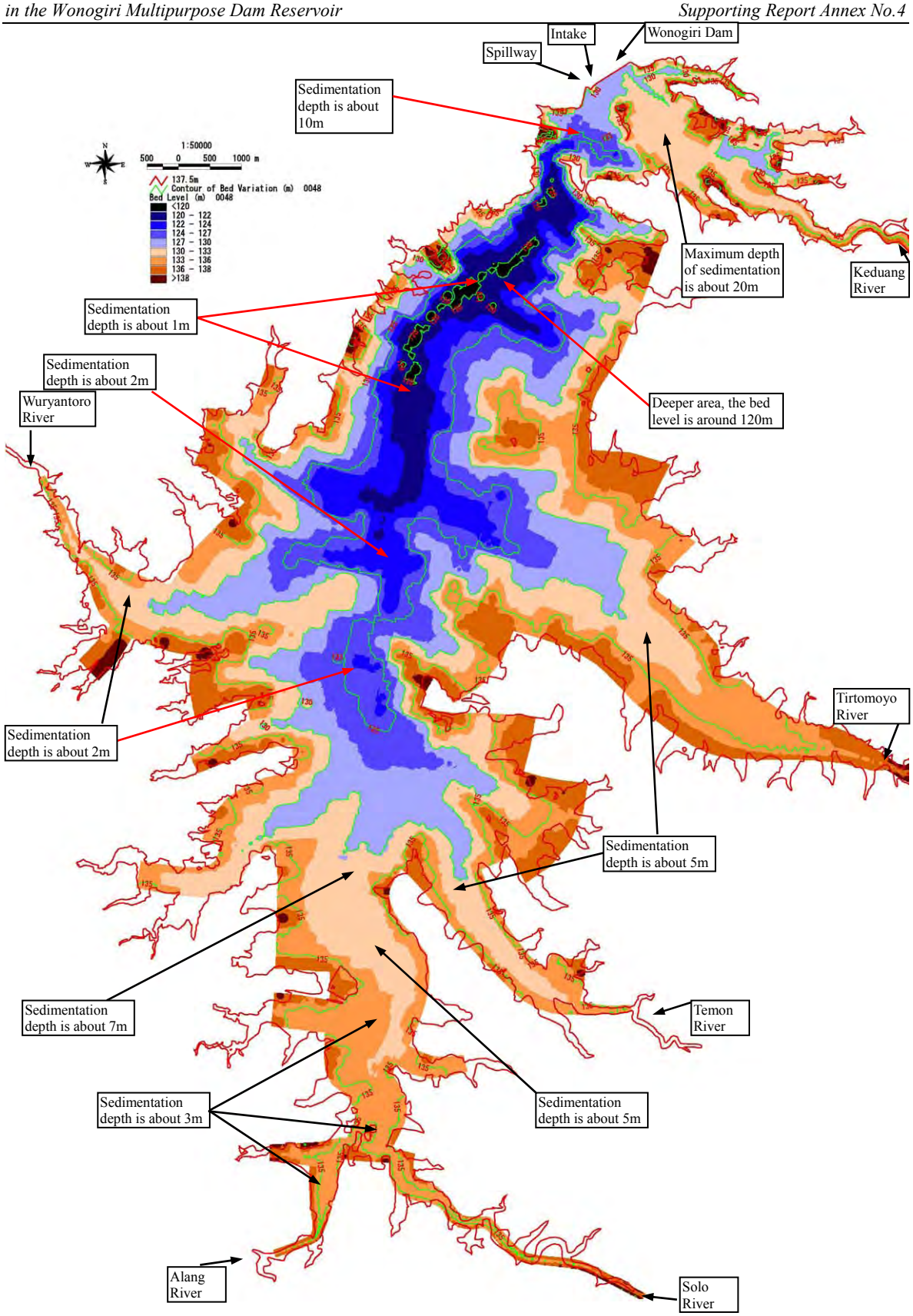

Figure 3.4.1 Bed Level Contour in the Reservoir (Measured in October 2004, Contour Unit: m)

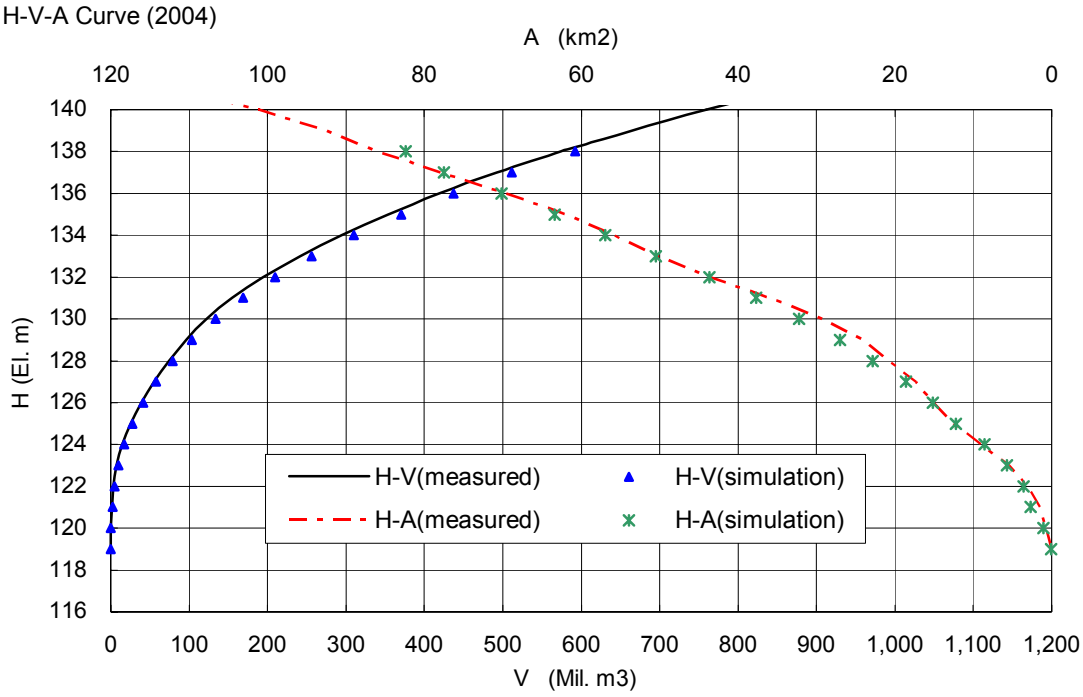

Figure 3.4.2 H-A and H-V Curves Based on Both the Measurement and the Simulation in the Reservoir (October 2004)

(2) Water Inflow and Outflow

Flow discharge hydrographs in the main inflow rivers are specified as the water inflow condition (Figure 3.3.1~3.3.7). During the rainy season of 2004-2005, maximum flood occurred on 3 December 2004 and the peak discharge of total inflow was about 1,330 m^3/s. Much more floods occurred in Keduang River.

Water release through the intake is specified as the water outflow condition (Figure 3.3.8). During the season, the spillway was not run because the inflow was less than that in the average year.

(3) Sediment Inflow and Outflow

Sediment inflow from each river is specified according to equation (2.27) and the parameters in Table 3.3.2, and its particle size distribution according to Table 3.3.3.

Sediment release (outflow) from the Wonogiri reservoir through both the spillway and the intake of hydropower plant is estimated by the outflow discharge of water and the computational concentration of SS near the facilities. It should be specially emphasized that the computational bottom concentration is employed for the concentration releasing from the intake.

3.4.2 Computational Results

(1) Water Level

The measured water level (chain line) in the reservoir and the computational one (solid line) by NKhydro2D model are compared in Figure 3.4.3. It shows a quite good agreement between the measurement and the computation with maximum difference about 0.1m. The difference is less than 0.05m even near the end of the rainy season.

(2) Velocity

Velocity vectors and contours at peak of several major floods are shown in Figure 3.4.4 - 3.4.7. The peak discharge of major flood in the inflow river is listed in Table 3.4.2.

Table 3.4.2 Peak Discharge (m^3/s) of Major Flood during the Rainy Season of 2004-2005

Flood Peak Time	Keduang River	Tirtomoyo River	Temon River	Solo River	Alanag River	Residual	Total	Water Level
2004/12/03 /10:00	303.6	178.0	78.6	376.4	247.1	148.6	1332.2	131.0m
2005/03/13 /21:00	167.0	207.4	25.1	315.5	154.4	109.1	978.6	135.0m
2005/03/31 /20:00	113.3	219.0	59.7	303.4	248.9	118.5	1062.8	136.0m

The flow velocity in river area was fast during flood, while that in center of the reservoir was very much slowly, about 1cm/s or below. The velocity in the center become more slowly with rising of the water level. Furthermore, counter flow to the center from the dam area due to flood in Keduang River occurred, especially when water level of the reservoir was lower. This inevitably affects sediment transport and sedimentation in the area.

Trajectory of flood flow (muddy current) near the dam is shown in the following Photo. Comparing the velocity contours in Figure 3.4.6 and 3.4.7 with this trajectory of muddy current (Photo 3.4.1 and 3.4.2), it is understood that the flow pattern by the simulation is consistent with the field observation.

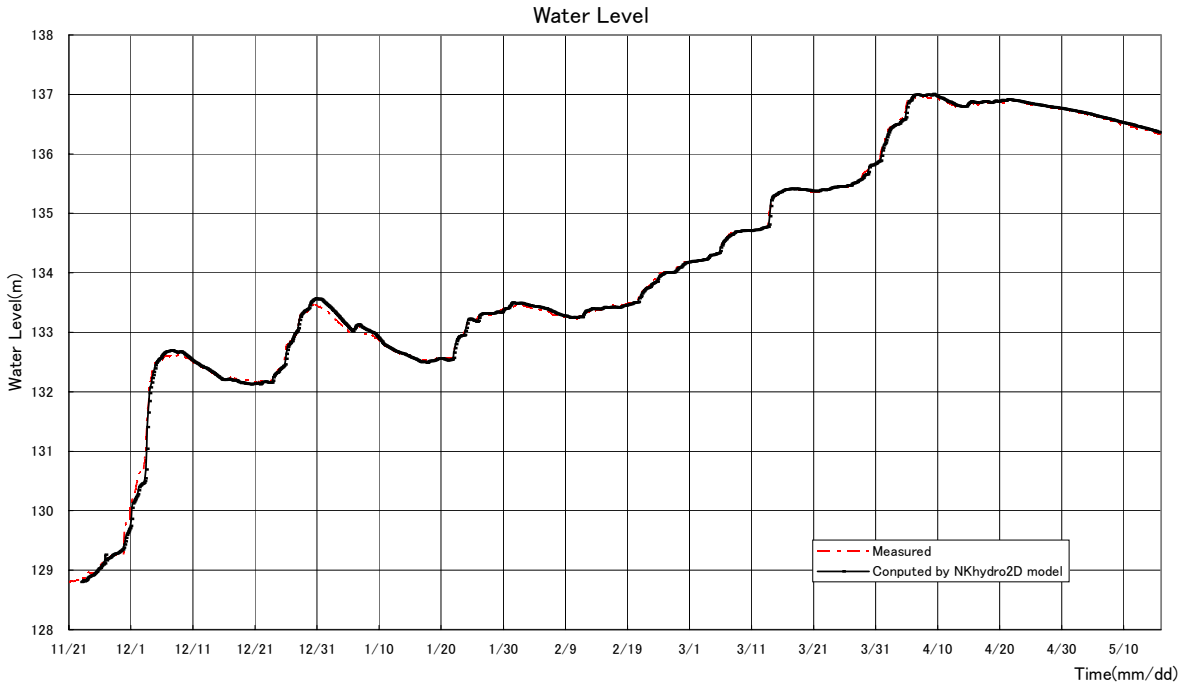

Figure 3.4.3 Measured and Computed Water Level in the Reservoir (2004-2005)

Trajectory of Flood Flow (Muddy Current) in the Reservoir

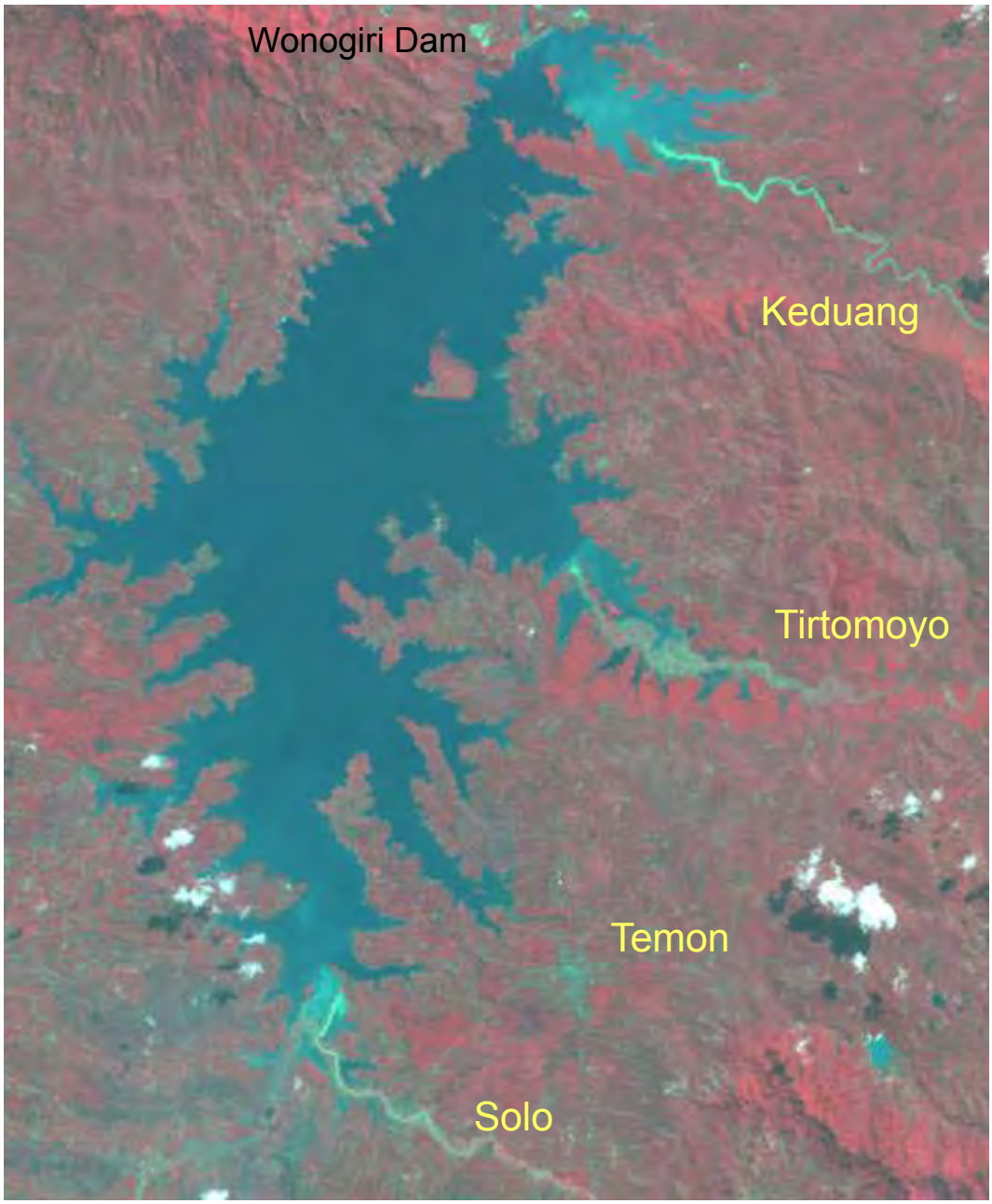

Satellite Photo during Flood (Muddy Current) in the Reservoir

(3) SS Concentration

Concentration of suspended sediment (SS) at flood peak of December 3, 2004 and after 2 days of the flood in the reservoir is shown in Figure 3.4.8 and 3.4.9. It is found that the concentration in river area during flood was higher and the muddy current was inversely transported into the center of the reservoir from Keduang River, which is consistent with the trajectory of the main flow (the above Photo). After the flood, concentration of SS in the center increased while that in river area declined.

Both the measured and the computed SS concentration in the intake during the period of November 23, 2004 ~ May 15, 2005 are shown in Figure 3.4.10. Though there is a deviation in the time, the computed SS concentration almost corresponds to the observation.

(4) Sedimentation and Trap Ratio of the Reservoir

Computational variation of bed level in the reservoir during November 2004 - May 2005 is shown in Figure 3.4.11. During the rainy season of 2004 - 2005, sedimentation in the river area (fore-set bed) was about 0.1 ~ 0.3m, while that in the center of the reservoir was less than 0.02m. By the results, it is understood that much sedimentation occurred in the river area (top-set and fore-set bed) and the sedimentation progressed gradually to the center of the reservoir (bottom-set bed) from the river area.

Computational sedimentation volume in different area (Figure 3.2.1) is listed in Table 3.4.3. As that in Table 3.2.1, Keduang area consists of Keduang and Dam area in Figure 3.2.1. Comparisons of computational particle size distribution with the measurement of the sedimentation are shown in Figure 3.4.12~3.4.18. By comparing the computation (Table 3.4.3) with the measurement (Table 3.2.1), the following conclusions are obtained.

- The computational sedimentation volume (2,255,000 m^3, deposition base) is consistent with the measurement (2,317,000m^3). The difference is possibly caused by the difference between the simulation period and the measurement (the former is a little bit shorter than the latter).
- Distribution of the computational sedimentation agrees with the measurement.
- Computational particle size distribution of the sedimentation is also in good agreement with the measurement (Figure 3.4.12~3.4.18), especially in Keduang area, Temon area and Solo&Alang area, the computation is almost the same as the measurement. In Center area, Tirtomoyo area and CenterUP area, computation of the distribution for finer material is the same as the measurement, though there is a little bit difference between the computation of distribution for coarser material and the measurement.

Sediment supply with inflow in the rivers and sediment transport volume through the confluence section of the rivers during the rainy season of 2004 - 2005 are shown in Figure 3.4.19 - 3.4.27. Locations of the sections are shown in Figure 3.1.1. Herein, the transported volume of sediment is in deposition base. The averaged dry density of the bed material in the reservoir is 1,064 kg/m^3 and the density of soil is about 2,650 kg/m^3. Minus volume of transported sediment in Figure 3.4.20 means that sediment was transported to the center of the reservoir from Keduang River.

Volume of transported volume through Section No.4 and No.1 is shown in Figure 3.4.28 and 3.4.29. Minus volume of transported sediment in Figure 3.4.29 means that sediment was transported to the center of the reservoir from the downstream side (Keduang River area).

- Most of the sediment supplied from the rivers, especially the coarser one, deposited in the river area, and the sediment transported into the center of the reservoir was little. There was only little sediment, the deposition volume 1,400 m^3, to be transported from Keduang (Dam) area to Center area. This means that there was almost no sediment exchange between Keduang area and the upstream area in the season.
- About 110,000 m^3 of total supplied sediment 410,000 m^3 was transported into the center of the reservoir from Tirtomoyo River (Figure 3.4.21 and 3.4.22). Almost all the sediment supplied from Temon river (about 85,000 m^3) deposited in the Temon river area (Figure 3.4.23 and 3.4.24).
- About 440,000 m^3 of total supplied sediment 840,000 m^3 was transported into the center from Solo River as well as Alang River (Figure 3.4.25 – 3.4.27).

- By the results of Figure 3.4.28 and 3.4.29, it is understood that there is a cross section between the section No.1 and No.4, through which the transport volume of sediment should be 0 during the rainy season of 2004-2005. Therefore, the effect on the sedimentation in the area near the Wonogiri dam site of the sediment transporting from the upstream area (Bengawan Solo river, Alang river, Temon river, Tirtomoyo river, Wuryantoro river, etc.) can almost be ignored. During the major floods, sediment with the counter flow was transported through section No.1 into the center of the reservoir from Keduang River area.

Computational sediment release through the intake of hydropower plant is 141,000m^3 (Figure 3.4.30), almost clay only (particle size < 0.005mm) except that at lower water level of the reservoir. The sediment release during January 5 ~ May 15, 2005 is 86,000m^3 which is approximately equal to the observation (71,300 m^3).

Sediment inflow and outflow of the reservoir is listed in Table 3.4.4. It shows that most of the sediment inflow is fine material that is called as clay with the size less than 0.005mm. Only about 10% of the sediment inflow is coarser with the size greater than 0.075mm. Sediment trap ratio by the reservoir (Table 3.4.4, based on the total inflow) was 94%, in which the trap ratio of clay was 91% while the silt and the coarser were almost trapped completely.

However, the above analysis has shown that only little sediment, supplied from the upstream area of the reservoir, reached to the dam area. It is better to calculate the trap ratio by the sediment supplied from Keduang River only. With the basis of sediment from Keduang River, the trap ratio of clay reduced to 74~76%, although the silt and the coarser were almost all trapped (Table 3.4.5). It is found that larger amount of the sediment from Keduang River was released to the downstream by the intake. This is important for evaluation of countermeasures against the sedimentation.

Table 3.4.3 Computational Sedimentation during the Rainy Season of 2004-2005 (Deposition Base, m^3)

Area	Sedimentation Volume (m3)	Sediment Distribution (%)								
		d= 0.0013mm	0.0013~ 0.005mm	0.005~ 0.016mm	0.016~ 0.031mm	0.031~ 0.075mm	0.075~ 0.25mm	0.25~ 0.85mm	0.85~ 2.0mm	2.0~ 19.0mm
Keduang	668,100	59.87	5.55	10.59	8.48	7.00	6.33	2.05	0.15	0.00
Tirtomoyo	300,800	50.23	6.14	8.04	8.82	8.12	8.72	6.69	2.79	0.46
Temon	120,200	63.49	7.06	9.78	6.31	7.74	4.73	0.78	0.12	0.00
Solo&Alang	396,800	58.42	6.06	11.73	8.16	8.48	5.01	1.89	0.25	0.00
CenterUP+ Wuryantoro3	447,300	52.11	4.84	15.85	11.40	9.32	3.59	2.15	0.63	0.11
Center	202,500	80.40	9.00	9.38	1.22	0.00	0.00	0.00	0.00	0.00
Wuryantoro	93,800	53.91	4.59	6.66	6.04	8.38	11.01	7.00	2.04	0.37
Wuryantoro2	25,400	56.17	4.81	6.63	5.63	7.79	10.23	6.50	1.90	0.34
Total	2,254,900									

Table 3.4.4 Computational Sediment Transport Balance and Trap Ratio by the Reservoir during the Rainy Season of 2004-2005 (Based on Total Sediment Inflow)

Location	Sediment Transport Volume (m3)	Sediment Transport Volume with Different Size (m3)								
		d= 0.0013mm	0.0013- 0.005mm	0.005- 0.016mm	0.016- 0.031mm	0.031- 0.075mm	0.075- 0.25mm	0.25- 0.85mm	0.85- 2.0mm	2.0- 19.0mm
Keduang River	811,000	527,100	50,500	72,800	56,800	46,800	42,400	13,700	1,000	0
Tirtomoyo River	409,000	235,700	29,400	29,400	28,300	26,000	27,900	21,400	8,900	1,500
Temon River (supply)	85,000	41,800	5,100	9,500	8,700	11,400	7,100	1,200	200	0
Solo River (supply)	506,000	290,000	24,700	82,000	49,600	41,800	12,300	4,700	700	0
Alang River (supply)	335,000	213,400	26,200	39,500	24,300	19,400	8,900	3,100	500	0
Residual (Wuryantoro, etc.) (supply)	246,000	137,900	11,900	16,300	13,900	19,200	25,200	16,000	4,700	900
PowerPlant (release)	−141,000	−125,600	−13,300	−2,000	−100	0	0	0	0	0
Trap Ratio	0.94	0.91	0.91	0.99	1.00	1.00	1.00	1.00	1.00	1.00

Table 3.4.5 Computational Sediment Transport Balance and Trap Ratio by the Reservoir during the Rainy Season of 2004-2005 (Based on Sediment Inflow of Keduang River)

Location	Sediment Transport Volume (m3)	Sediment Transport Volume with Different Size (m3)								
		d= 0.0013mm	0.0013- 0.005mm	0.005- 0.016mm	0.016- 0.031mm	0.031- 0.075mm	0.075- 0.25mm	0.25- 0.85mm	0.85- 2.0mm	2.0- 19.0mm
Keduang River	811,000	527,100	50,500	72,800	56,800	46,800	42,400	13,700	1,000	0
PowerPlant (release)	−141,000	−125,600	−13,300	−2,000	−100	0	0	0	0	0
Trap Ratio	0.83	0.76	0.74	0.97	1.00	1.00	1.00	1.00	1.00	1.00

3.4.3 Conclusion of the Simulation for Calibration

The above analyses show that estimation of sediment inflow and its allocation to the rivers during the rainy season of 2004 ~ 2005 is reasonable, and NKhydro2D model can be employed to simulate the sedimentation in Wonogiri reservoir. The following conclusions are obtained.

- The sediment inflow was 2,452,000m^3 (deposition base), in which the sedimentation was 2,317,000m^3 during the season. The sediment transport rate in the rivers can be estimated as a function of discharge (equation (2.27) and Table 3.3.2).
- The flow velocity in river area was fast during flood, while that in the center of the reservoir was very much slowly.
- Counter flow to the center due to the flood in Keduang River occurred. This feature was consistent with the observed trajectory of flood flow (muddy current) near the dam.
- SS concentration in river area during flood was higher and the muddy current was inversely transported into the center of the reservoir from Keduang River.
- Much sedimentation occurred in the river area (mouth) and the sedimentation progressed gradually to the center of the reservoir. During the rainy season of 2004 - 2005, sedimentation in the river area was about 0.1-0.3m, while that in the center of the reservoir was less than 0.02m.
- There was only little sediment, the deposition volume 1,400 m^3, to be transported from Keduang (Dam) area to Center area. This means that there was almost no sediment exchange between Keduang area and the upstream area in the season.

- The computational sediment release during the rainy season of 2004 - 2005 through the intake was about 141,000 m^3, almost clay only (particle size < 0.005mm). The measured release was about 135,000 m^3.
- With the basis of sediment from Keduang River, the trap ratio of clay by the reservoir was 74~76%, although silt and the coarser were almost all trapped.

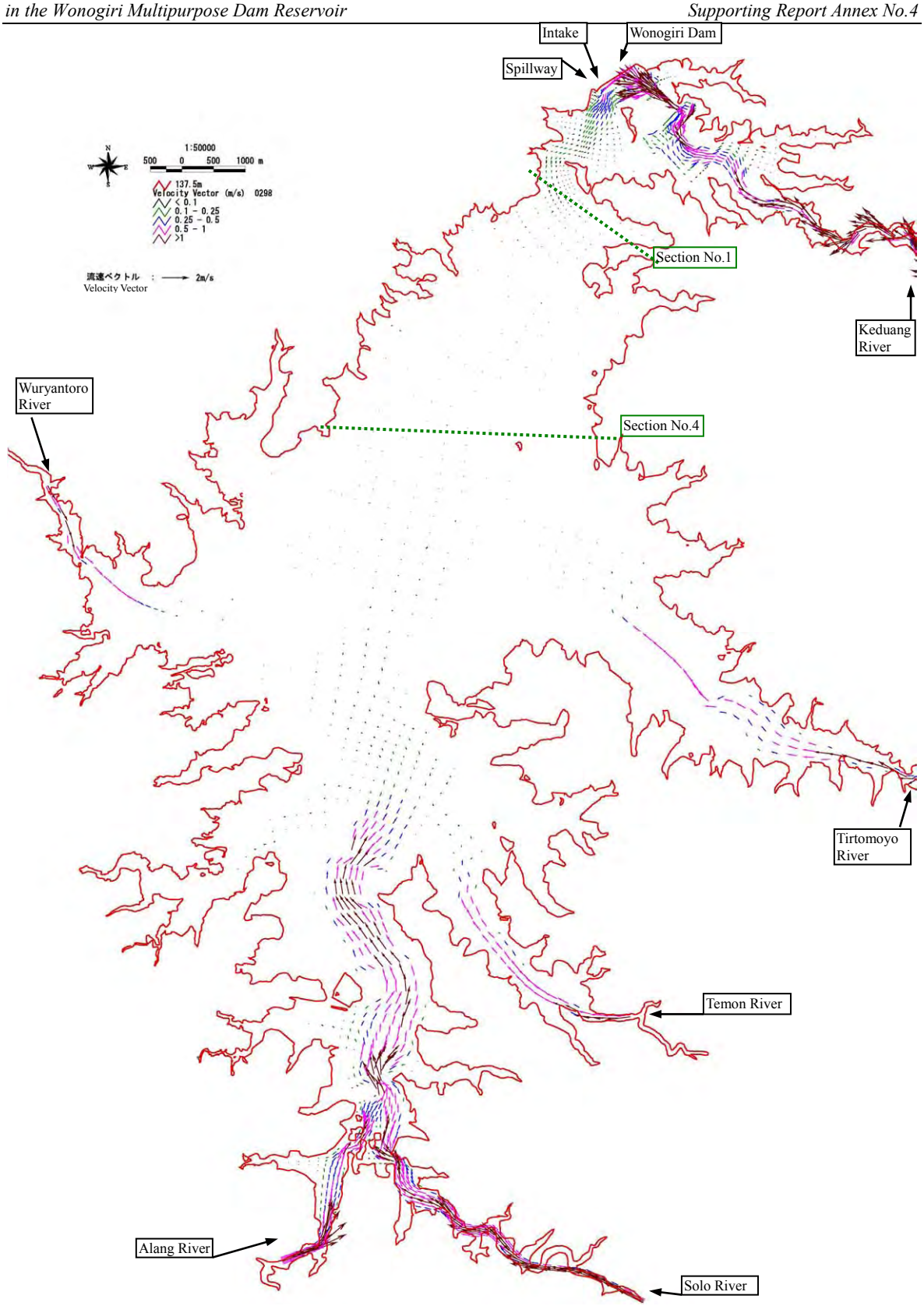

Figure 3.4.4 Computational Velocity Vector in the Reservoir at the Flood Peak Occurred on December 3, 2004 (Water Level = 131m)

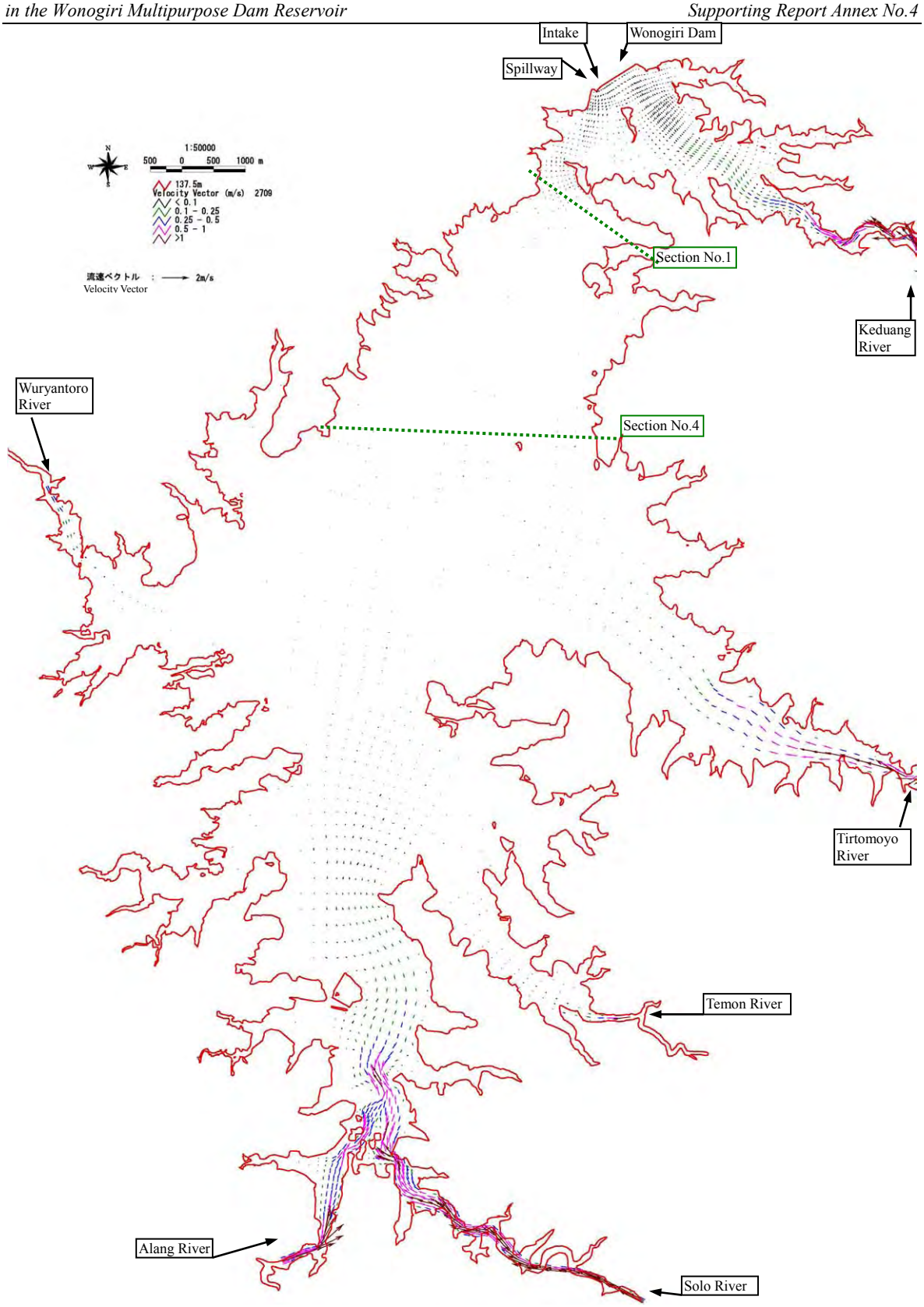

Figure 3.4.5 Computational Velocity Vector in the Reservoir at the Flood Peak Occurred on March 13, 2005 (Water Level = 135m)

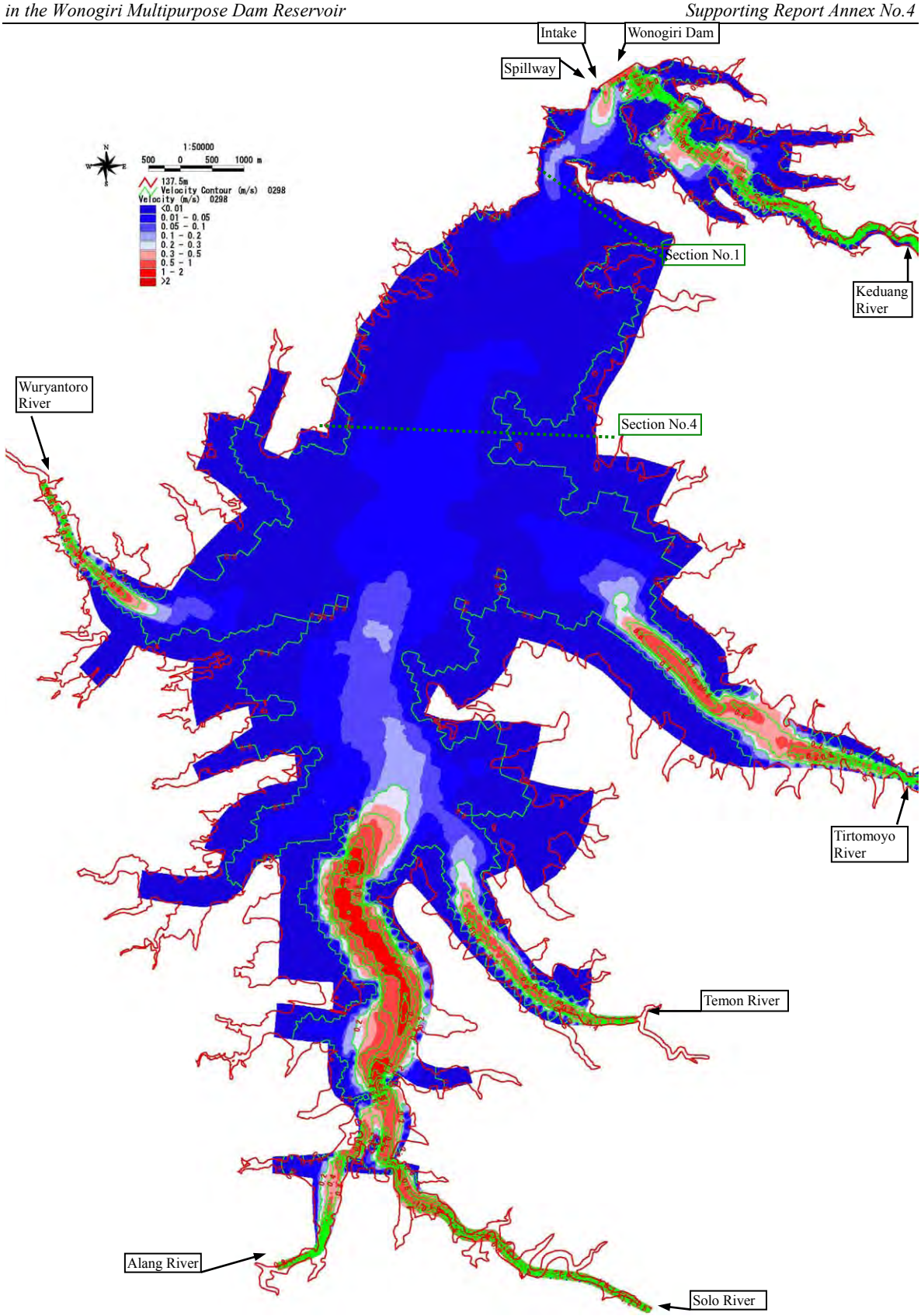

Figure 3.4.6 Computational Velocity Contour in the Reservoir at the Flood Peak Occurred on December 3, 2004 (Water Level = 131m, Contour Unit: m/s)

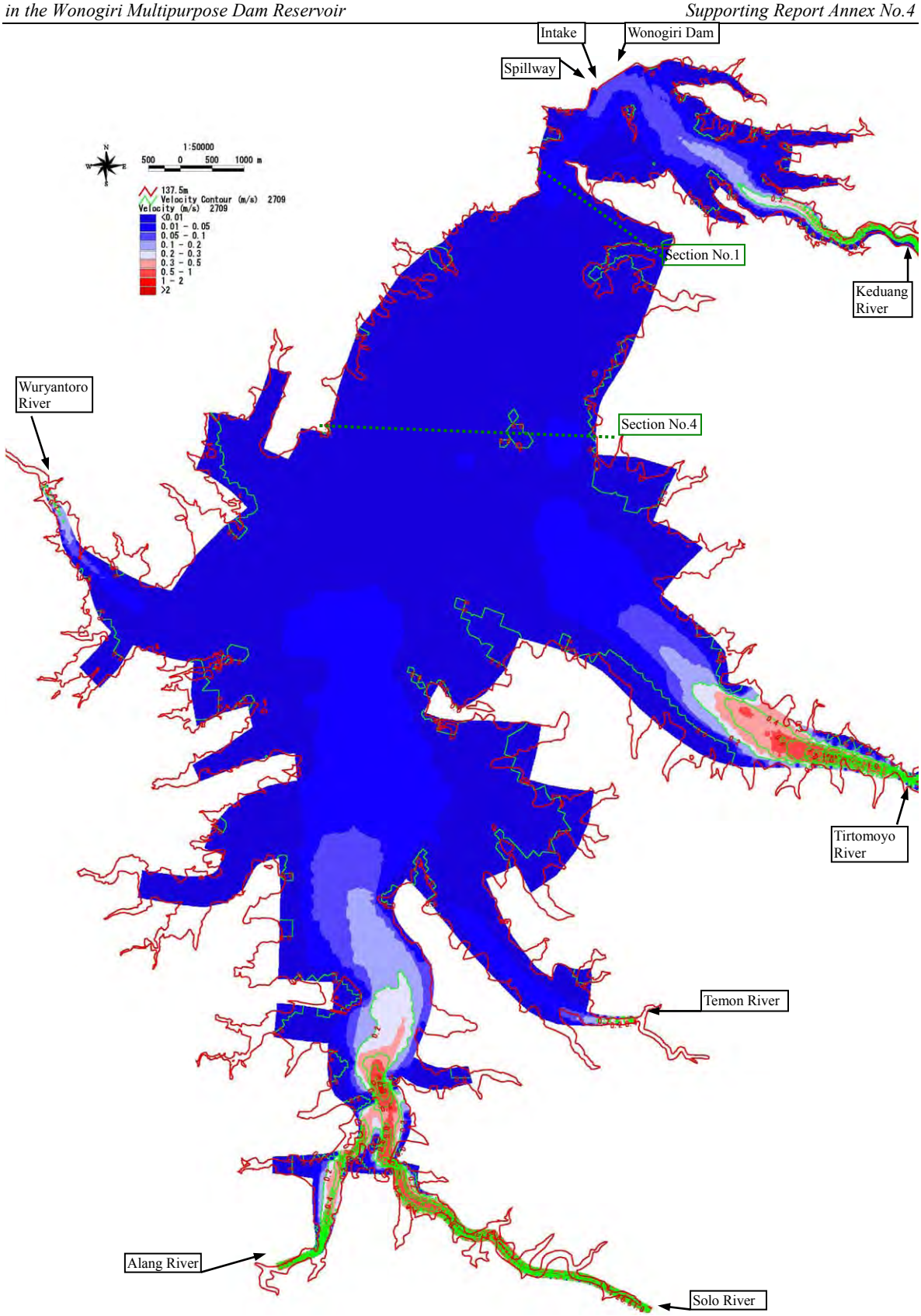

Figure 3.4.7 Computational Velocity Contour in the Reservoir at the Flood Peak Occurred on March 13, 2005 (Water Level = 135m, Contour Unit: m/s)

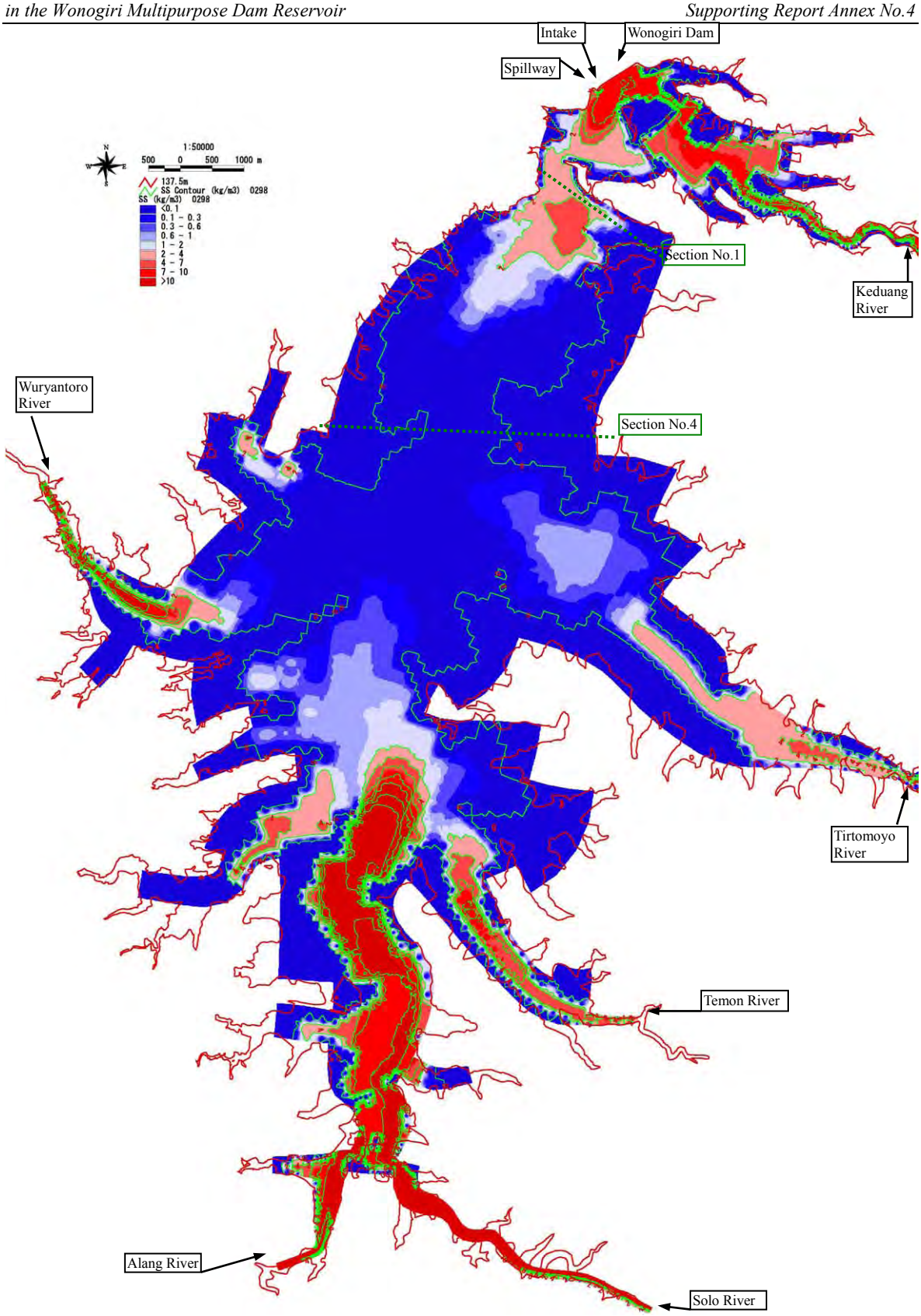

Figure 3.4.8 Computational Concentration of Suspended Sediment in the Reservoir at the Peak of Flood on December 3, 2004 (Water Level=131m, Contour Unit: kg/m^3)

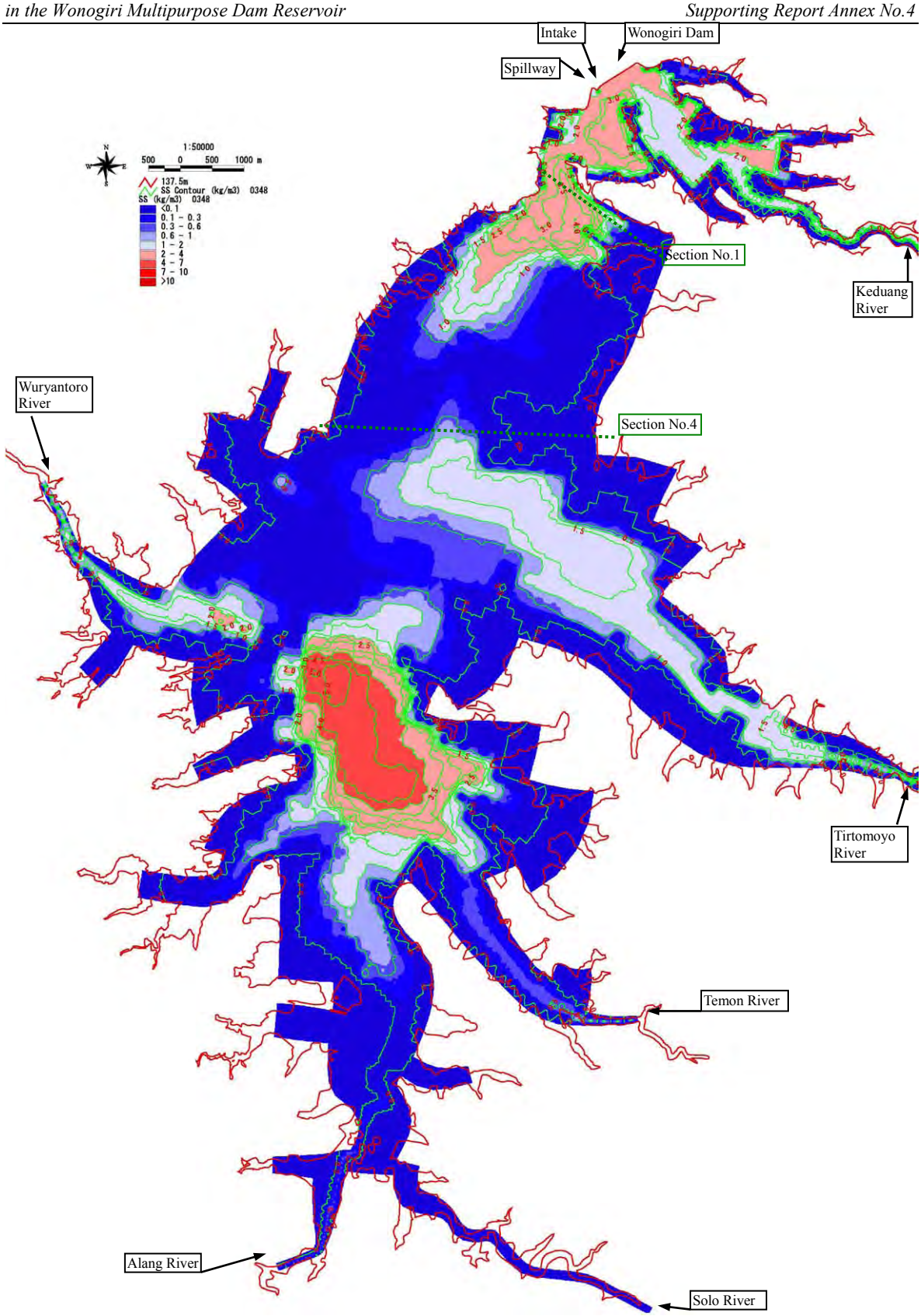

Figure 3.4.9 Computational Concentration of Suspended Sediment in the Reservoir on December 5, 2004 (after 2 days of the flood on December 3, Water Level=132.5m, Contour Unit: kg/m^3)

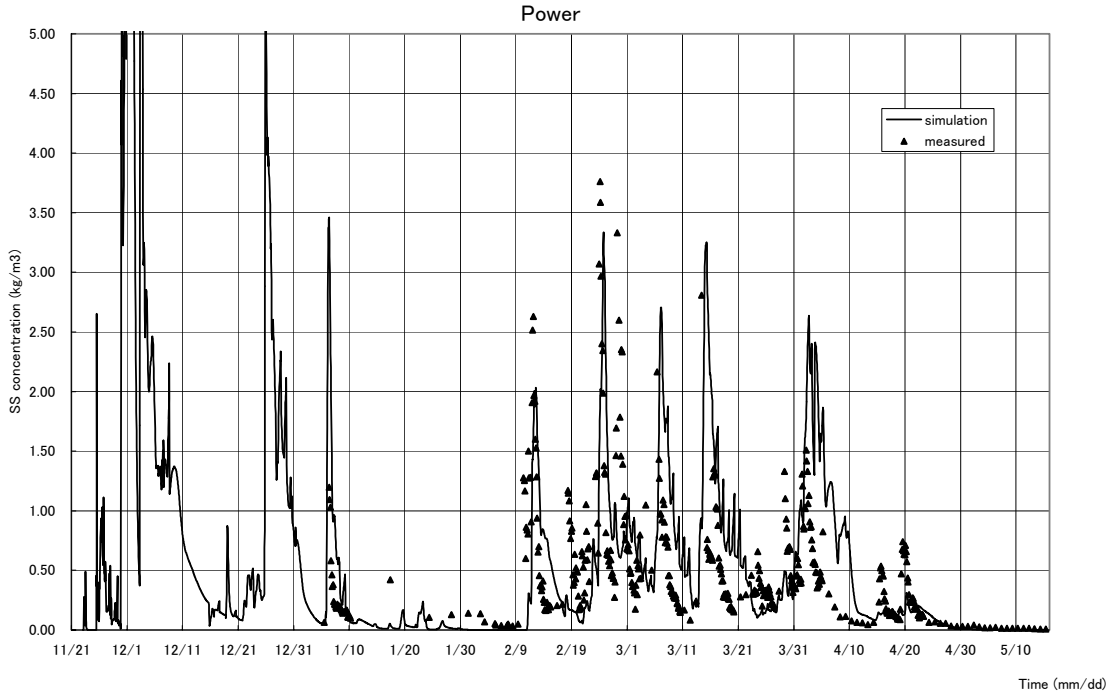

Figure 3.4.10 The Measured and the Computed Concentration of SS in the Intake during Nov.23,2004 – May 15, 2005

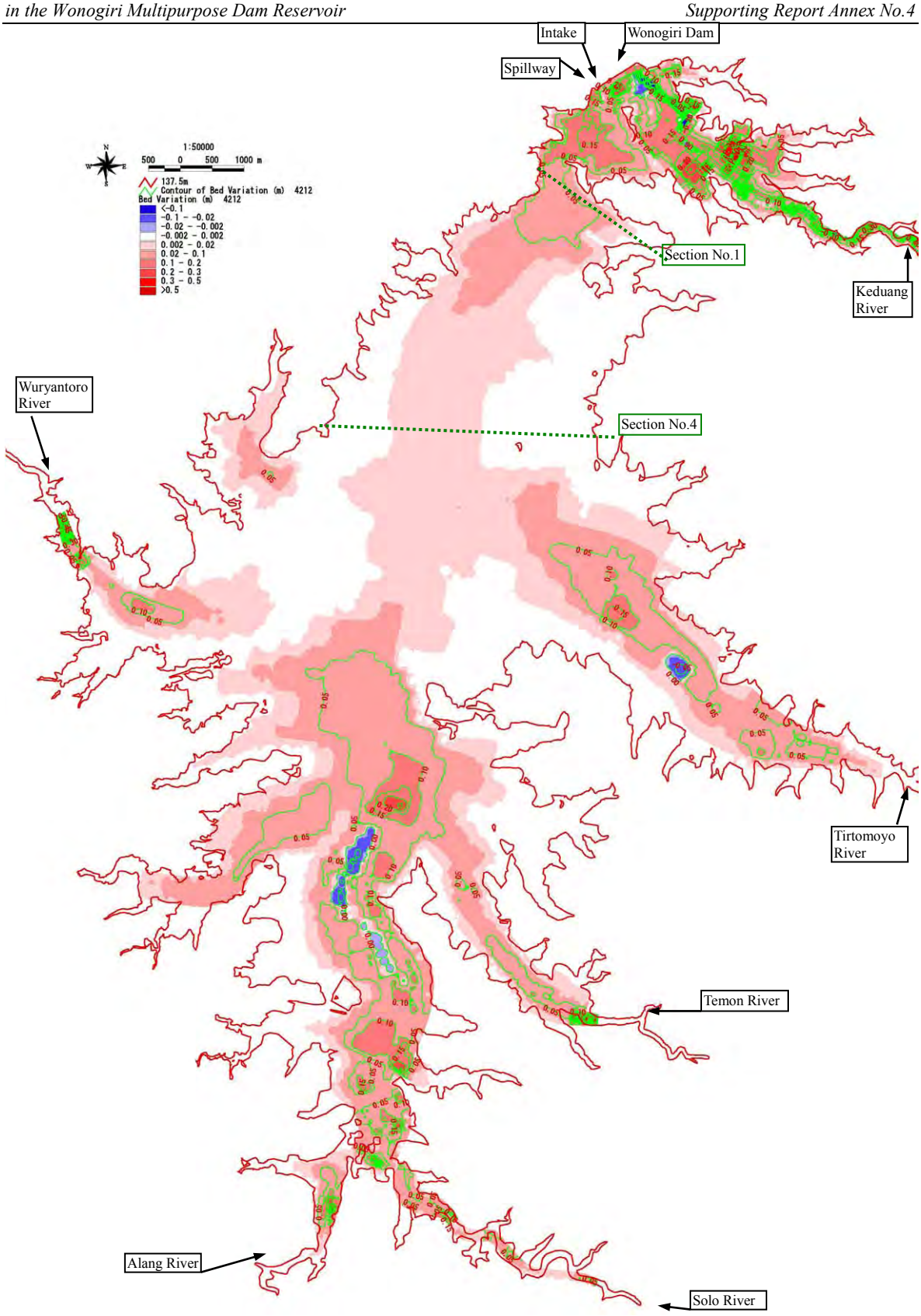

Figure 3.4.11 Computational Bed Level Variation in the Reservoir at the End of Rainy Season of 2004 - 2005 (Contour Unit: m)

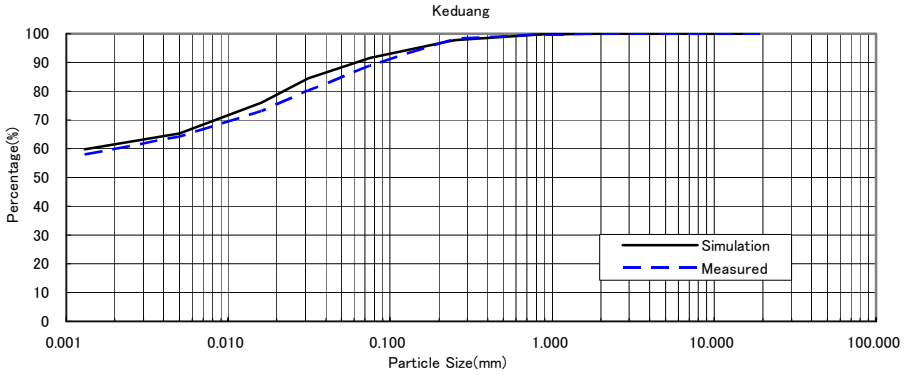

Figure 3.4.12 Comparison of Computational Particle Size Distribution with the Measurement of the Sedimentation in Keduang Area of the Reservoir (Rainy Season of 2004 - 2005)

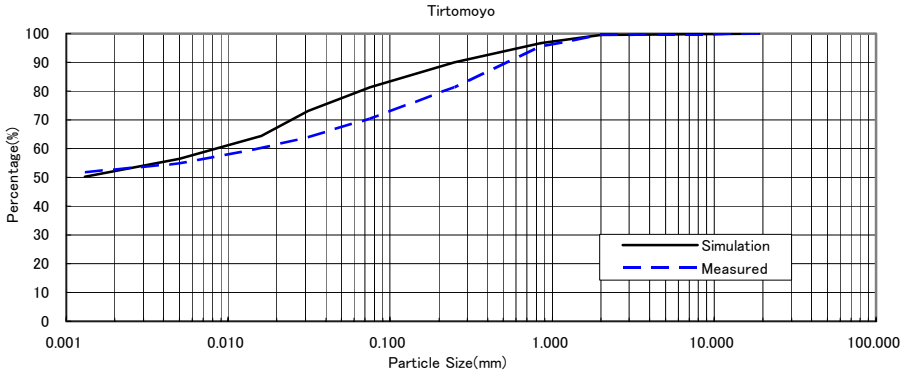

Figure 3.4.13 Comparison of Computational Particle Size Distribution with the Measurement of the Sedimentation in Tirtomoyo Area of the Reservoir (Rainy Season of 2004 - 2005)

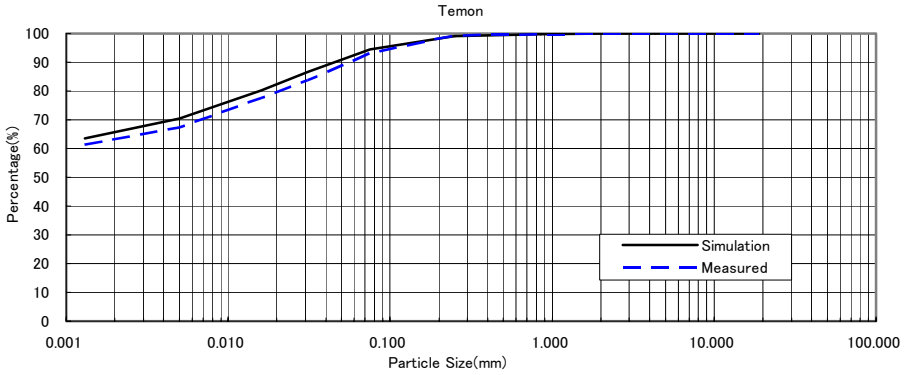

Figure 3.4.14 Comparison of Computational Particle Size Distribution with the Measurement of the Sedimentation in Temon Area of the Reservoir (Rainy Season of 2004 - 2005)

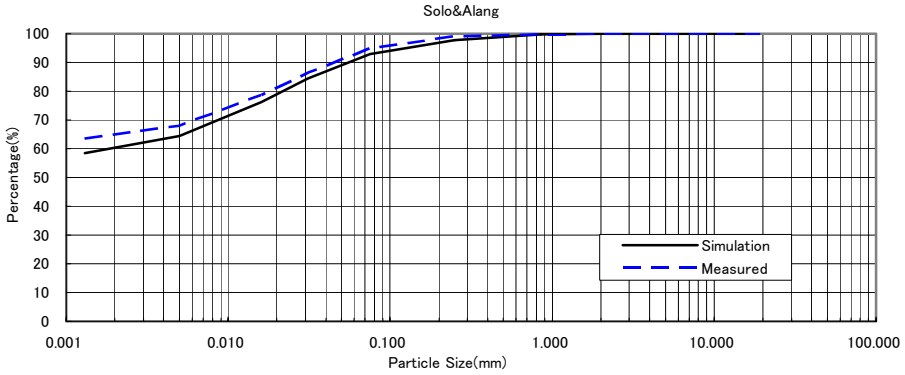

Figure 3.4.15 Comparison of Computational Particle Size Distribution with the Measurement of the Sedimentation in Solo&Alang Area of the Reservoir (Rainy Season of 2004 - 2005)

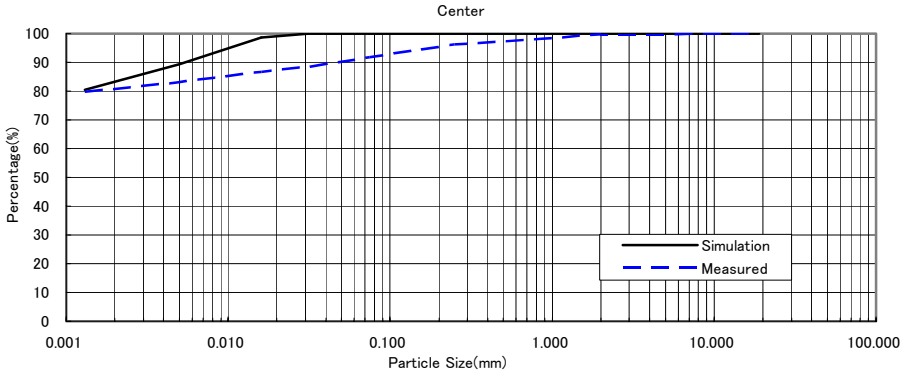

Figure 3.4.16 Comparison of Computational Particle Size Distribution with the Measurement of the Sedimentation in Center Area of the Reservoir (Rainy Season of 2004 - 2005)

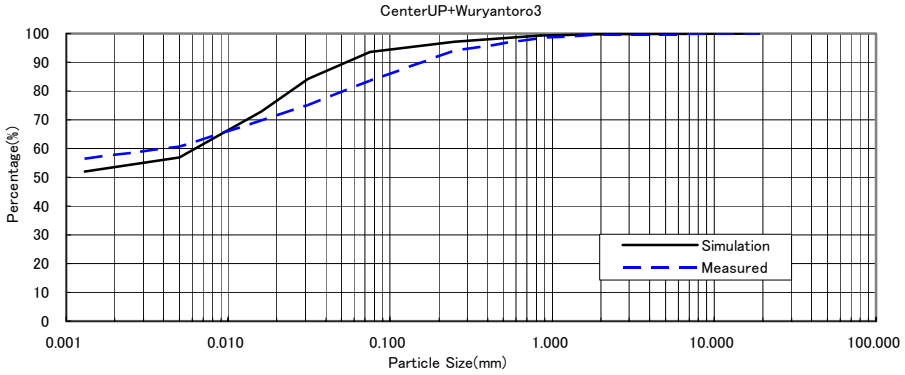

Figure 3.4.17 Comparison of Computational Particle Size Distribution with the Measurement of the Sedimentation in CenterUP&Wuryantoro3 Area of the Reservoir (Rainy Season of 2004 - 2005)

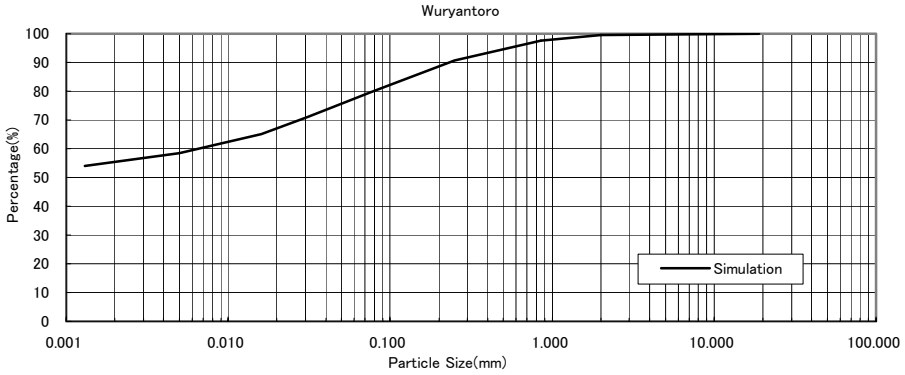

Figure 3.4.18 Computational Result of Particle Size Distribution of the Sedimentation in Wuryantoro Area of the Reservoir (Rainy Season of 2004 - 2005)

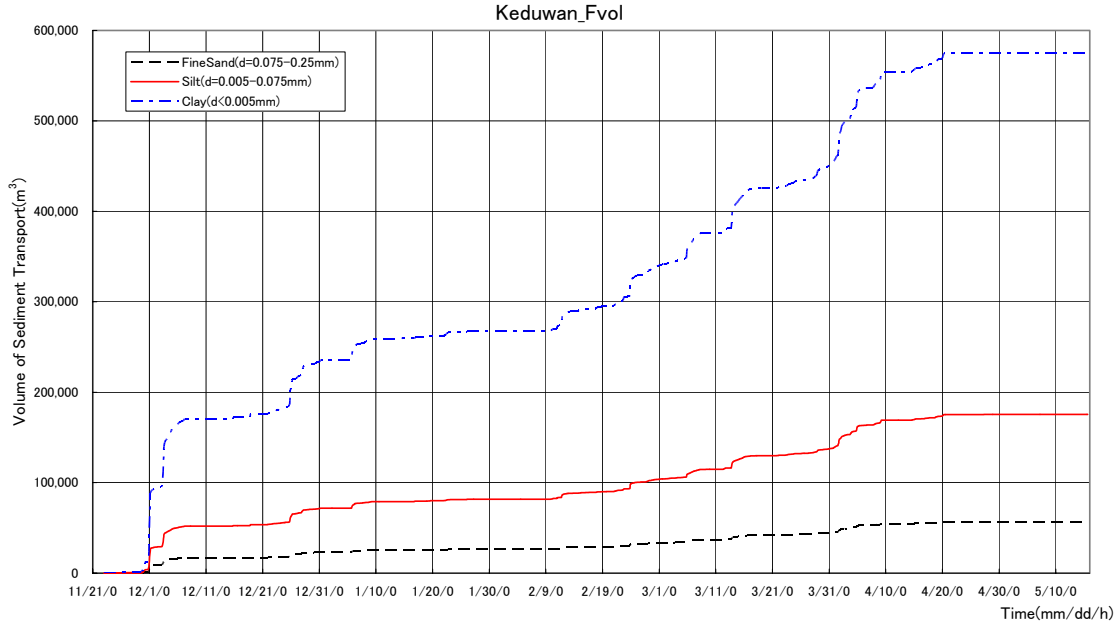

Figure 3.4.19 Transport Volume of SS in Keduang River (2004/11/23-2005/5/15, Deposition Base, m^3)

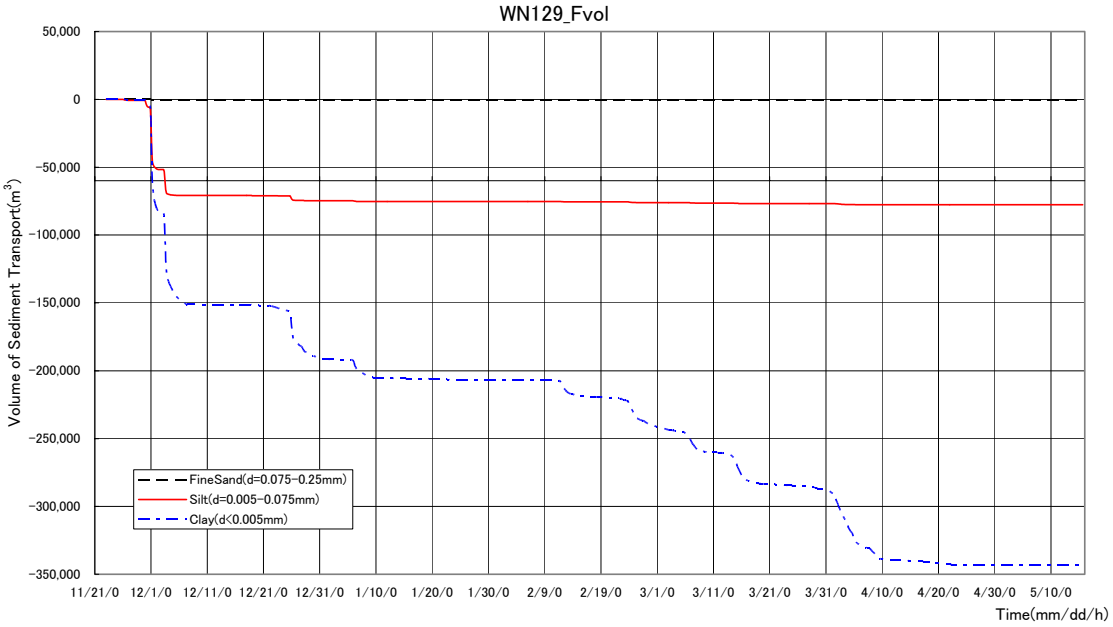

Figure 3.4.20 Transport Volume of SS at Keduang Exit (2004/11/23-2005/5/15, Deposition Base, m^3)

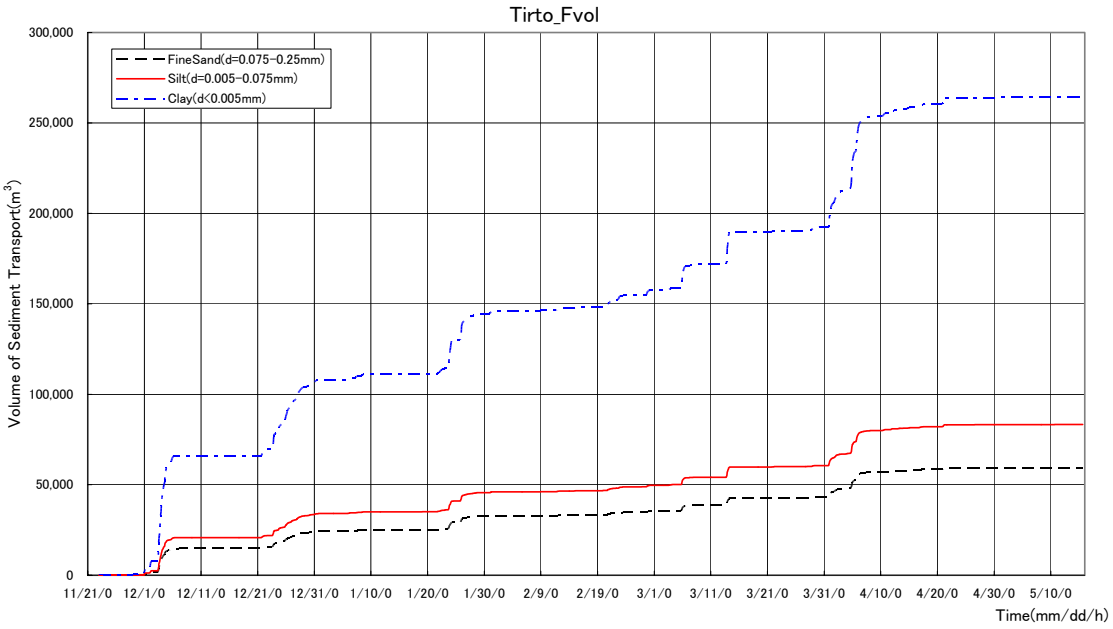

Figure 3.4.21 Transport Volume of SS in Tirtomoyo River (2004/11/23-2005/5/15, Deposition Base, m^3)

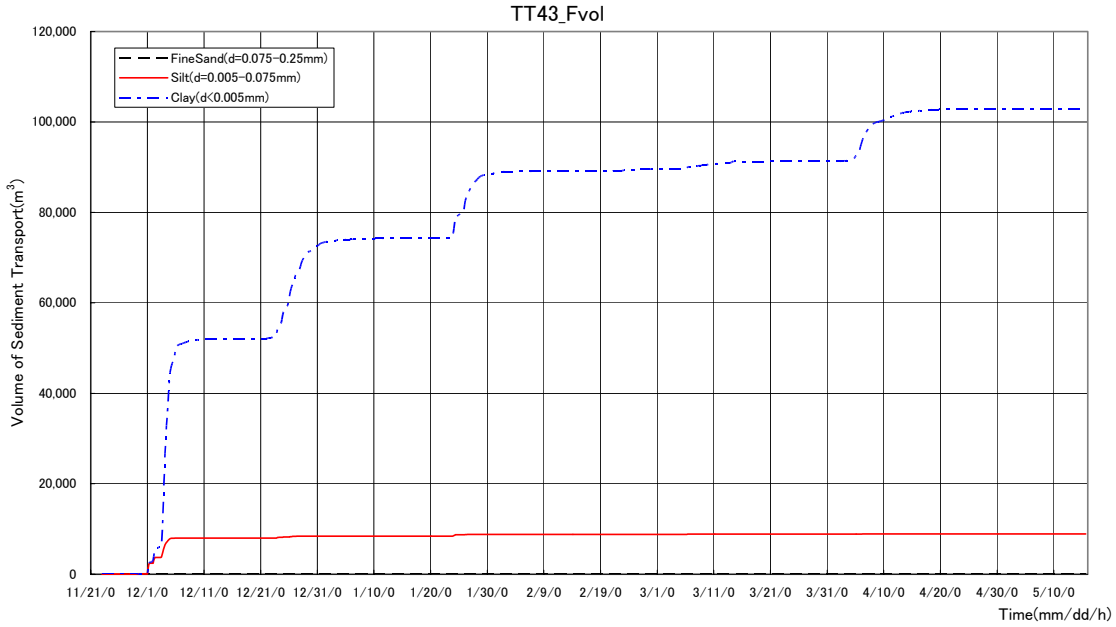

Figure 3.4.22 Transport Volume of SS at Tirtomoyo Exit (2004/11/23-2005/5/15, Deposition Base, m^3)

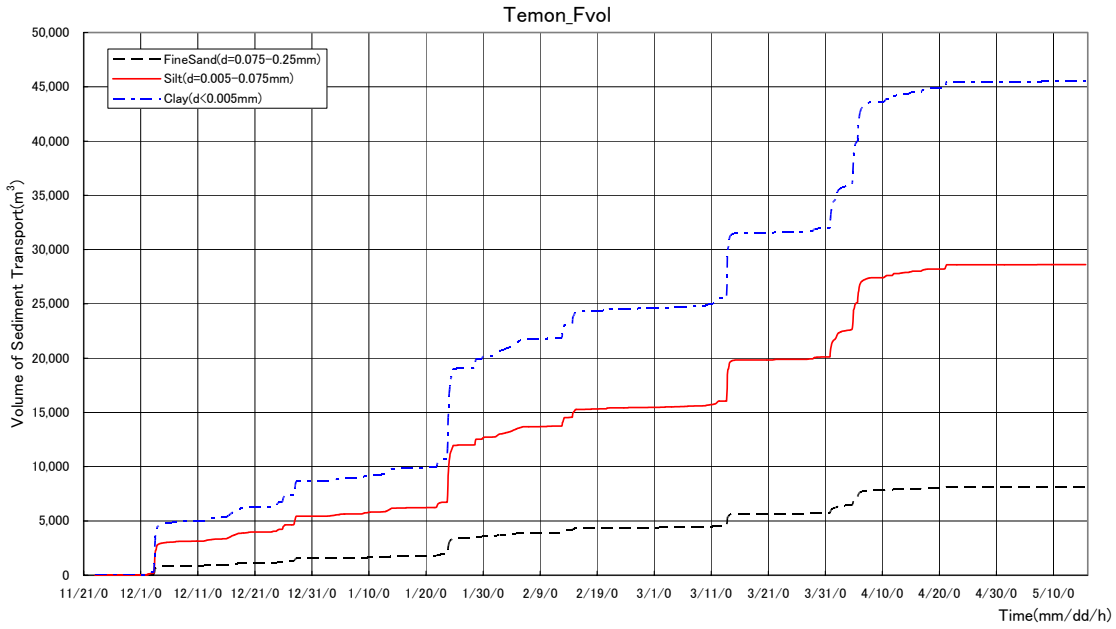

Figure 3.4.23 Transport Volume of SS in Temon River (2004/11/23-2005/5/15, Deposition Base, m^3)

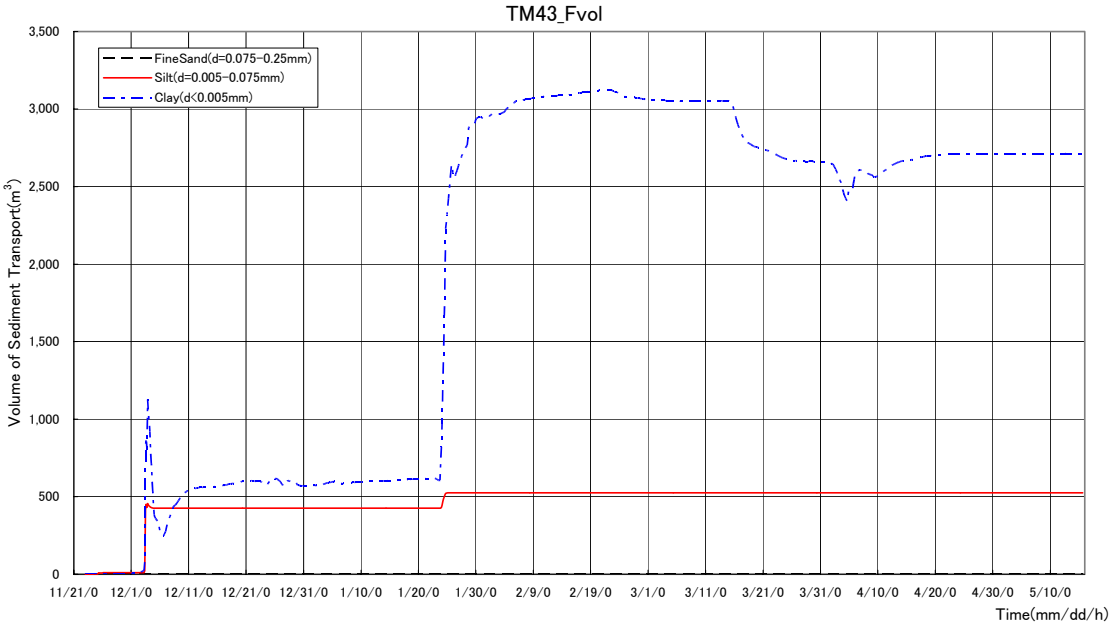

Figure 3.4.24 Transport Volume of SS at Temon Exit (2004/11/23-2005/5/15, Deposition Base, m^3)

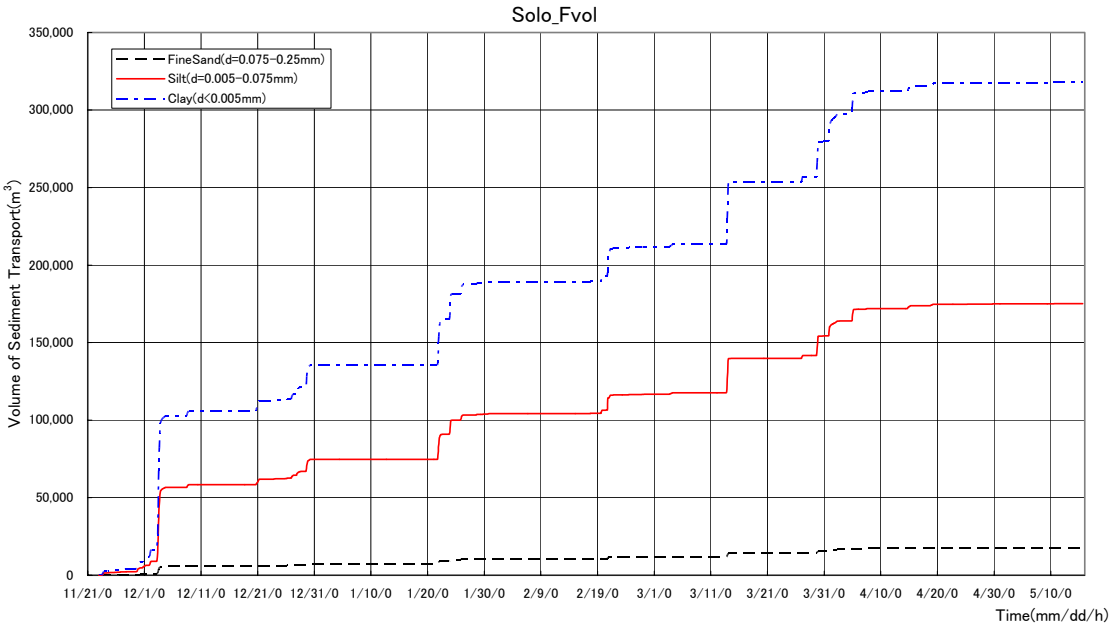

Figure 3.4.25 Transport Volume of SS in Solo River (2004/11/23-2005/5/15, Deposition Base, m^3)

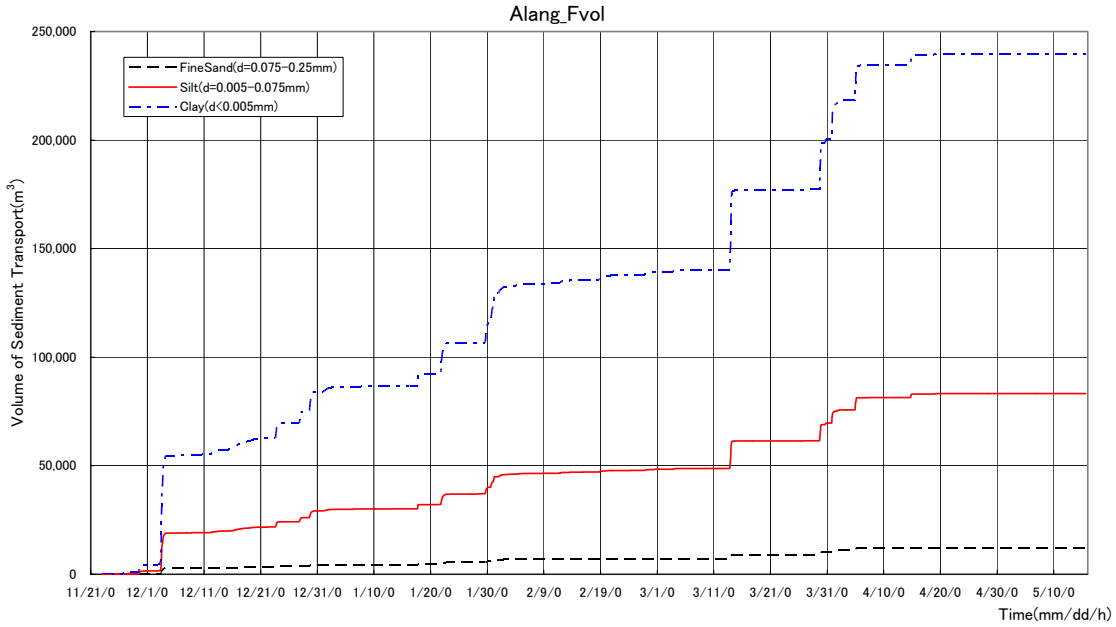

Figure 3.4.26 Transport Volume of SS in Alang River (2004/11/23-2005/5/15, Deposition Base, m^3)

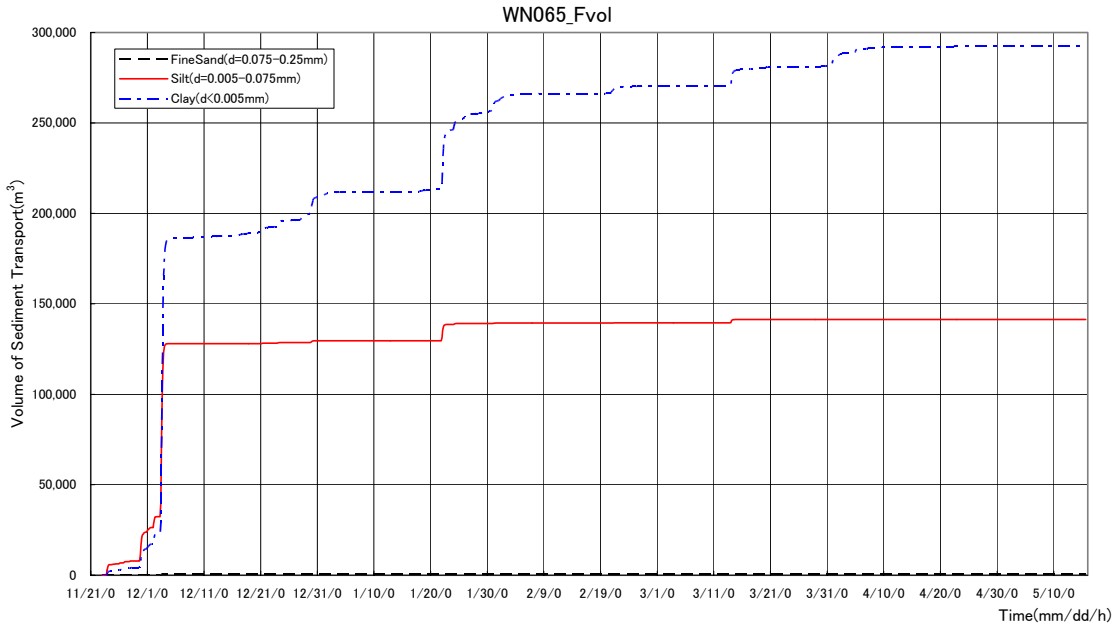

Figure 3.4.27 Transport Volume of SS at Solo&Alang River (2004/11/23-2005/5/15, Deposition Base, m^3)

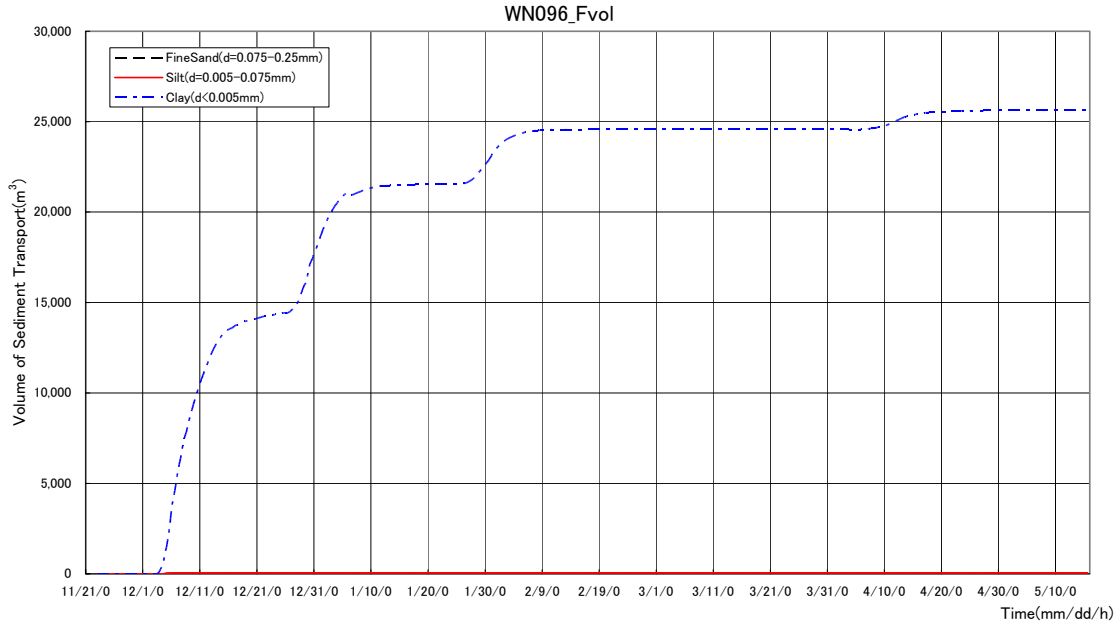

Figure 3.4.28 Transport Volume of SS through Section No.4 (2004/11/23-2005/5/15, Deposition Base, m^3)

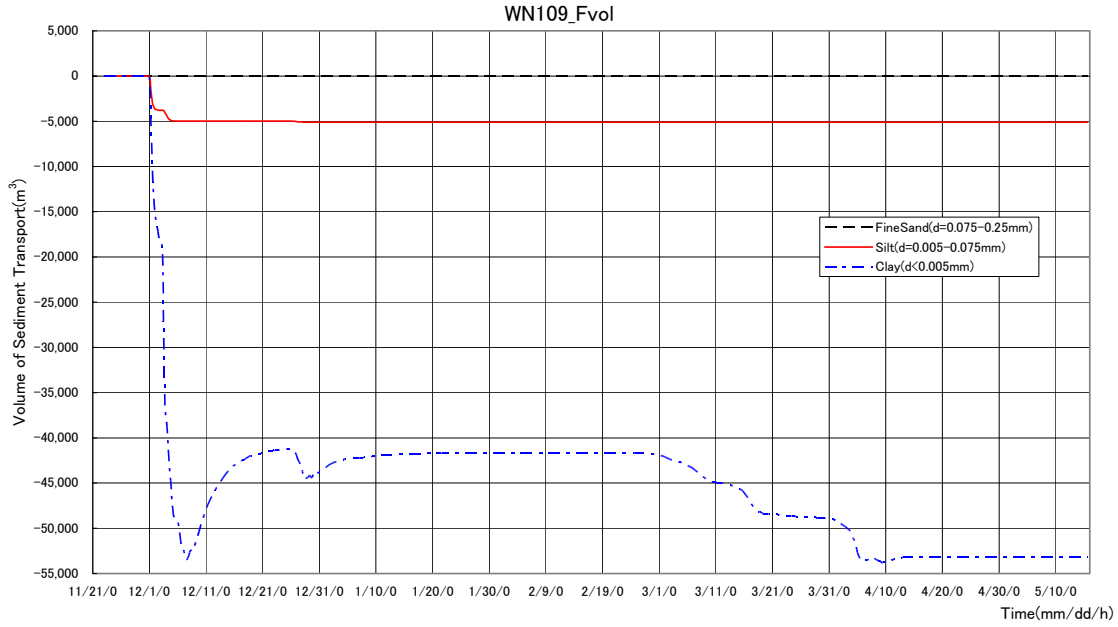

Figure 3.4.29 Transport Volume of SS through Section No.1 (2004/11/23-2005/5/15, Deposition Base, m^3)